



# High-resolution land-use land-cover change data for regional climate simulations over Europe - Part I: The plant functional type basemap for 2015

Vanessa Reinhart<sup>1,2</sup>, Peter Hoffmann<sup>1,2</sup>, Diana Rechid<sup>1</sup>, Jürgen Böhner<sup>3</sup>, and Benjamin Bechtel<sup>4</sup>

<sup>1</sup>Helmholtz-Zentrum Hereon, Climate Service Center Germany (GERICS), Fischertwiete 1, 20095 Hamburg, Germany

<sup>2</sup>Universität Hamburg, Institut of Geography, Section Physical Geography, Bundesstraße 55, 20146 Hamburg, Germany

<sup>3</sup>Universität Hamburg, Institute of Geography, Cluster of Excellence “Climate, Climatic Change, and Society” (CLICCS), 805A Geomatikum, Bundesstraße 55, D-20146, Hamburg, Germany

<sup>4</sup>Ruhr-Universität Bochum, Department of Geography, Universitätsstraße 150/ Gebäude IA, 44801 Bochum, Germany

**Correspondence:** Vanessa Reinhart (vanessa.reinhart@hereon.de)

**Abstract.** The concept of plant functional types (PFTs) is shown to be beneficial in representing the complexity of plant characteristics in land use and climate change studies using regional climate models (RCMs). By representing land use and land cover (LULC) as functional traits, responses and effects of specific plant communities can be directly coupled to the lowest atmospheric layers. To meet the requirements of RCMs for realistic LULC distribution, we developed a PFT dataset for Europe (LANDMATE PFT Version 1.0; Reinhart et al., 2021b). The dataset is based on the high-resolution ESA-CCI land cover dataset and is further improved through the the additional use of climate information. Within the LANDMATE PFT dataset, satellite-based LULC information and climate data are combined to achieve the best possible representation of the diverse plant communities and their functions in the respective regional ecosystems while keeping the dataset most flexible for application in RCMs. Each LULC class of ESA-CCI is translated into PFT or PFT fractions including climate information by using the Holdridge Life Zone concept. Through the consideration of regional climate data, the resulting PFT map for Europe is regionally customized. A thorough evaluation of the LANDMATE PFT dataset is done using a comprehensive ground truth database over the European Continent. A suitable evaluation method has been developed and applied to assess the quality of the new PFT dataset. The assessment shows that the dominant LULC groups, cropland and woodland, are well represented within the dataset while uncertainties are found for some less represented LULC groups. The LANDMATE PFT dataset provides a realistic, high-resolution LULC distribution for implementation in RCMs and is used as basis for the LUCAS LUC dataset introduced in the companion paper by Hoffmann et al. (submitted) which is available for use as LULC change input for RCM experiment setups focused on investigating LULC change impact.



## 1 Introduction

20 Land use and land cover (LULC), including the vegetation type and function, was declared an Essential Climate Variables (ECVs) by the Global Climate Observing System (GCOS) (Bojinski et al., 2014). Changes in ECVs are crucial factors of climate change and therefore need to be monitored and further represented in climate models to be able to assimilate and understand atmospheric processes and feedback effects on different scales. For LULC, anthropogenic modifications are the most important drivers of change. De- and reforestaion and expansion of urban and cropland areas affect biogeophysical (e.g.,  
25 albedo, roughness, evapotranspiration, runoff) and biogeochemical (e.g., carbon emissions and sinks) surface properties and processes (Mahmood et al., 2014; Lawrence and Vandecar, 2015; Alkama and Cescatti, 2016; Perugini et al., 2017; Davin et al., 2020). Besides LULC changes, land management practices are being assessed regarding influence of related land surface modifications on regional climate, and also the potential of land management practices regarding climate change adaptation and mitigation efforts (Lobell et al., 2006; Kueppers et al., 2007; Burke and Emerick, 2016).

30 In order to represent impacts and feedbacks of LULC modifications as realistic as possible, regional climate models (RCMs) require an accurate representation of LULC and its changes. In this context, the concept of plant functional types (PFTs) is increasingly used for the representation of LULC in RCMs. A comprehensive review of the subsequent development of PFTs representing vegetation dynamics in climate models was done by Wullschleger et al. (2014). The need for applicable global PFT maps for vegetation models that are used with atmospheric models was already well emphasized by Box (1996).  
35 Moreover, the requirement that a climate model should include a vegetation model representing the biosphere was discussed by Lavorel et al. (2007). One criterion that is highly emphasized is the inter-regional applicability of a preferably simple PFT classification, which has the ability to capture key characteristics of the biosphere from biome to continental scale, regardless of climate zone and individual vegetation composition. A variety of PFT definitions and cross-walking procedures (CWPs), used for translating LULC products into global or regional PFT maps, are currently available. The European Space Agency  
40 Climate Change Initiative (ESA-CCI) and the United States Geological Service (USGS) provide the only two ready to use continuous global products to the community (Poulter et al., 2015; Sulla-Menashe and Friedl, 2018). However, the individual PFT definitions and CWPs as well as the mostly satellite based input data differ greatly in complexity and temporal and horizontal resolution (Bonan et al., 2002; Winter et al., 2009; Lu and Kueppers, 2012). Moreover, inter-regional consistency cannot be achieved by products that origin from regionally constrained input data or regionally adapted CWPs. Therefore,  
45 the additional use of climate information in the CWP from LULC to PFT is a highly useful step, to create a dynamically customizable product, that can be adapted to various climate and vegetation characteristics (Poulter et al., 2011).

With the present work, we introduce a PFT map for the European Continent that specifically addresses the requirements of the RCM community (Bontemps et al., 2013). The land cover maps of the ESA-CCI are translated into 16 PFTs creating an updated version of the interactive MOsaic-based Vegetation (iMOVE) PFTs that were originally developed for the RCM REMO  
50 (Wilhelm et al., 2014). Climate information is implemented into the CWP employing the Holdridge ecosystem classification concept based on the Holdridge Life Zones (HLZs; Holdridge et al., 1967), which provide a global classification of climatic zones in relation to potential vegetation cover. The HLZ concept is commonly used as a tool for ecosystem mapping from



various overlapping research communities (Lugo et al., 1999; Yue et al., 2001; Khatun et al., 2013; Szelepcsényi et al., 2014; Tatli and Dalfes, 2021). This paper gives a detailed documentation on the preparation of the PFT map - hereinafter referred to as "LANDMATE PFT" - within the Helmholtz Institute for Climate Service Science (HICSS) project "Modelling human LAND surface Modifications and its feedbacks on local and regional climate" (LANDMATE). The LANDMATE PFT map is prepared in close collaboration with the EURO-CORDEX Flagship Pilot Study Land Use and Climate Across Scales (FPS LUCAS; Rechid et al., 2017). Within the FPS LUCAS, RCM experiments are coordinated among an RCM ensemble to investigate the impact of LULC change for past climate and future climate scenarios. Through creation of LANDMATE PFT and the time series LUCAS LUC (Hoffmann et al., submitted), the need for improved LULC and LULC change representation among the FPS LUCAS RCM ensemble is met. For the preparation of LANDMATE PFT, we developed a CWP for the translation of LULC classes of ESA-CCI into 16 PFTs according to the needs of regional climate modellers from all over Europe (Bontemps et al., 2013). A key issue to address in the map development process is the accuracy of LULC representation in the final product (Hartley et al., 2017). In order to assess the quality of the product, we compared the LANDMATE PFT map to a comprehensive ground truth database for large parts of the European Continent. The quality information derived from the assessment supports the RCM community in addressing and interpreting uncertainties caused by LULC representation in RCMs. The general workflow and subsequently all utilized datasets are summarized in section 2 while the major steps of the CWP are listed in section 3. Section 4 introduces in detail the accuracy assessment procedure followed directly by the results in section 4.3. All CWTs and figures corresponding to the CWP and the accuracy assessment can be found in Appendix A and B.

## 2 Methods and data

The LANDMATE PFT map (Reinhart et al., 2021b) is a combination of multiple datasets and concepts created using well-established methods and in addition, by considering the expertise of regional climate modellers from all over Europe within the FPS LUCAS.

### 2.1 General workflow

The workflow to generate the LANDMATE PFT map is summarized in fig. 1, which also includes the steps to generate the LUCAS LUC dataset further described in the companion paper by Hoffmann et al. (submitted). First, the ESA-CCI land cover map (Sect. 2.2.1), which has a native resolution of  $\sim 300$  m, is aggregated to the  $0.1^\circ$  target resolution using SAGA GIS (Conrad et al., 2015). The target resolution results from the FPS LUCAS ensemble resolution (i.e., EURO-CORDEX domain EUR-11) that is used for LULC change impact studies in FPS LUCAS Phase II. The LULC type information from the original product is preserved in fractions per  $0.1^\circ$  grid cell which is advantageous to common majority resampling methods. The sum of PFT fractions in the whole dataset remains the same in all target resolutions, only the distribution of fractions per grid cell changes depending on the target resolution.

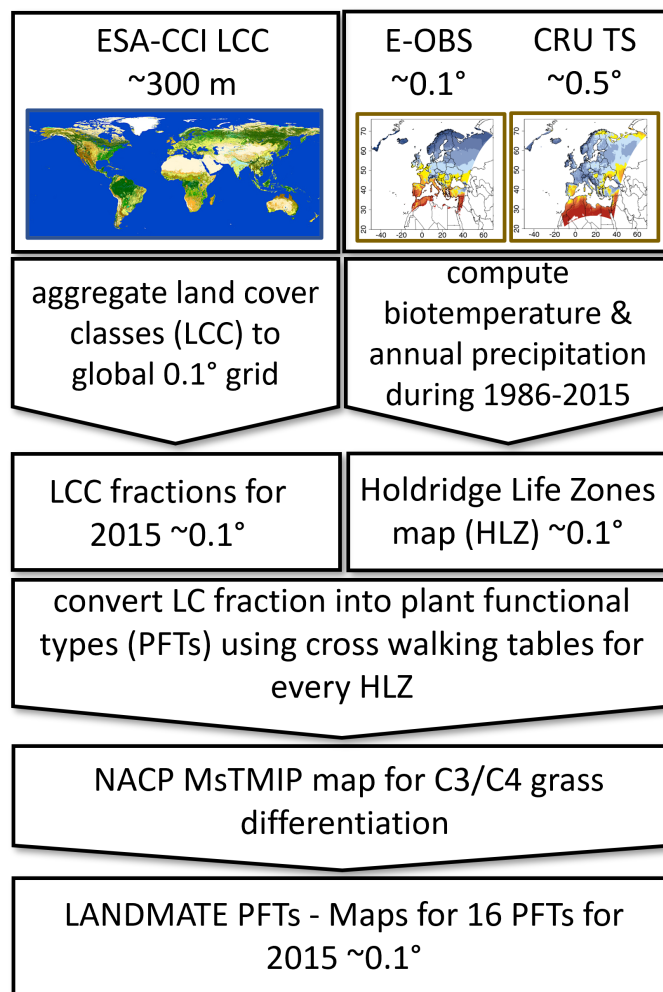


**Figure 1.** The general workflow to generate LANDMATE PFT 2015 Version 1.0. This workflow is part of the workflow to generate the LUCAS LUC time series as introduced in the companion paper by Hoffmann et al. (submitted)

The E-OBS gridded climate data (Sect. 2.2.2) is utilized for the preparation of the HLZ map over Europe (Sect. 2.2.4). From 85 E-OBS, the ensemble mean 2-meter-temperature and annual precipitation from 1950-2020 are used to create the HLZ map of 0.1° horizontal resolution which is further implemented in the CWTs to prepare the final LANDMATE PFT maps. For regions that are not covered by E-OBS, the respective data of the CRU dataset (Sect. 2.2.3) is used.

For each of the 37 ESA-CCI land cover classes, an individual CWT is created (Sect. 3) that includes a unique translation for each used HLZ. The translation process is based on Wilhelm et al. (2014) where the translation of the Global Land Cover 90 (GLC) 2006 to the 16 REMO-iMOVE PFTs is described. Since the nomenclature of GLC 2006 and ESA-CCI LC are similar and based on the same classification system some of the CWTs were initially adopted from (Wilhelm et al., 2014). For the more diverse ESA-CCI LC classes new CWTs need to be created. The new CWTs follow the translation of Poulter et al.



(2015) (ESA-CCI PFTs) but were carefully revised and modified during the process. This revision of the CWTs is supported by reference data and visual satellite image interpretation. The quality of the LANDMATE PFT dataset is finally assessed by comparison to a comprehensive ground truth database (Sect. 4).

## 2.2 Datasets & concepts

### 2.2.1 ESA-CCI LC

The European Space Agency Climate Change Initiative (ESA-CCI) provides continuous global land cover maps (ESA-CCI LC) on ~300 m horizontal grid resolution. The ESA-CCI LC maps are available for download in annual time steps for the years 1992-2018 (ESA, 2017). The classification of the LC maps follows the United Nations Land Cover Classification System (UN-LCCS) protocol (Di Gregorio, 2005) and consists of 22 level 1 classes and 14 additional level 2 classes, which include regional specifications. More information on ESA-CCI LC data processing can be found at [maps.elie.ucl.ac.be/CCI/viewer/download/ESACCI-LC-Ph2-PUGv2\\_2.0.pdf](https://maps.elie.ucl.ac.be/CCI/viewer/download/ESACCI-LC-Ph2-PUGv2_2.0.pdf). An overview of the satellite missions involved in the production of ESA-CCI LC is given in table 1. Besides systematic global validation efforts (ESA, 2017; Hua et al., 2018), a few regional approaches investigated the quality of ESA-CCI LC over Europe (Vilar et al., 2019; Reinhart et al., 2021a).

**Table 1.** Satellite missions involved in the production of ESA-CCI LC according to ESA (2017)

Time period		Satellite product
Baseline	Production	MERIS FR/RR <sup>1</sup> global SR <sup>2</sup> composites
2003-2012		
1992-1999		Baseline 10-year global map; AVHRR <sup>3</sup> global SR composites for back-dating baseline
1999-2013		Baseline 10-year global map; SPOT-VGT <sup>4</sup> global SR composites for up and back-dating the baseline; PROBA-V <sup>5</sup> global SR composites at 300 m
2013-2015		Baseline 10-year global map; PROBA-V global SR composites at 1 km for years 2014 and 2015 for updating the baseline; PROBA-V time series at 300 m
Since 2016		Sentinel-3 OLCI and SLSTR <sup>6</sup> 7-day composites

<sup>1</sup>MEdium Resolution Imaging Spectrometer Full Resolution/Reduced Resolution (ESA, 2002)

<sup>2</sup>Surface Reflectance

<sup>3</sup>Advanced Very-High-Resolution Radiometer (Hastings and Emery, 1992)

<sup>4</sup>SPOT Vegetation satellite program (Maisongrande et al., 2004)

<sup>5</sup>Project for On-Board Autonomy - Vegetation (Dierckx et al., 2014)

<sup>6</sup>Ocean and Land Colour Instrument (OLCI) and Sea and Land Surface Temperature Radiometer (SLSTR) (Donlon et al., 2012)



## 2.2.2 E-OBS Climate data

The E-OBS dataset (Cornes et al., 2018) is a daily gridded observational dataset, derived from station observations from European countries covering the period from 1950 to 2020. The point observations are interpolated using a spline method with random perturbations in order to produce an ensemble of realizations. For the creation of the HLZs that are used for the conversion of ESA-CCI LC classes to PFTs (Section 2.2.5), the ensemble mean of the 2-meter-temperature (TG) and precipitation (RR) on a regular 0.1° grid from E-OBS version 19.0e is used. It covers most of Europe, some parts of the Middle East and a narrow strip of Northern Africa.

## 2.2.3 CRU

The Climate Research Unit (CRU) TS 4.03 dataset is a global gridded high-resolution climate dataset based on station observations produced and maintained by the CRU of the University of East Anglia (Harris et al., 2014). The dataset provides global monthly means of climate parameters at 0.5° resolution from 1901 to 2019. In order to achieve the target resolution of 0.1° for the global LANDMATE PFT maps, the CRU climate data is downscaled using bilinear interpolation. Following Hoffmann et al. (2016), distance-weighted interpolation was applied to the atmospheric observation dataset CRU to extrapolate the climate data to the coastlines of the ESA-CCI LC maps in order to compensate for the different land-sea-masks of the products. The CRU climate dataset was used within this application for regions where E-OBS is not available.

## 2.2.4 Holdridge Life Zones

The Holdridge Life Zone (HLZ) concept was initially developed in 1967 (Holdridge et al., 1967) to define all divisions of the global biosphere, depending on the relation of biotemperature (average of monthly temperature above 0°C; since plant activities are idle below freezing, all values below 0°C are adjusted to 0°C), mean annual precipitation and ratio of potential evapotranspiration to mean annual precipitation. By combining threshold values of biotemperature and annual rainfall, the 38 HLZs are created (Table 2). In the present analysis, the tropical and subtropical as well as the polar and subpolar HLZs are merged. Through the merging of the aforementioned HLZs, 30 individual HLZs in total are available for the creation of the European HLZ map (Fig. 2). The dynamic character of the specific quantitative ranges of the long-term means of the

**Table 2.** The Holdridge Life Zones following (Holdridge et al., 1967).

Bio-temperature [°C]	Precipitation [mm]					
	<125	125 to <250	250 to <500	500 to <1000	1000 to <2000	>2000
<3	Subpolar dry tundra	Subpolar moist tundra	Subpolar wet tundra	Subpolar rain tundra	-	-
3 to <6	Boreal desert	Boreal dry shrub	Boreal moist forest	Boreal wet forest	Boreal rain forest	-
6 to <12	Cool temperate desert	Cool temperate desert shrub	Cool temperate steppe	Cool temperate moist forest	Cool temperate wet forest	Cool temperate rain forest
12 to <18	Warm temperate desert	Warm temperate desert scrub	Warm temperate thorn steppe/woodland	Warm temperate dry forest	Warm temperate moist forest	Warm temperate wet/rain forest
18 to <24	Subtropical desert	Subtropical desert shrub	Subtropical thorny steppe/woodland	Subtropical dry forest	Subtropical moist forest	Subtropical wet/rain forest
>24	Tropical desert	Tropical desert shrub	Tropical thorny woodland	Tropical very dry forest	Tropical dry forest	Tropical moist/wet/rain forest

utilized climate parameters make the HLZ classification more flexible than other available global ecosystem classifications and



130 therefore makes the HLZs most suitable for the application presented in this article. In addition the requirement for input data is relatively low.

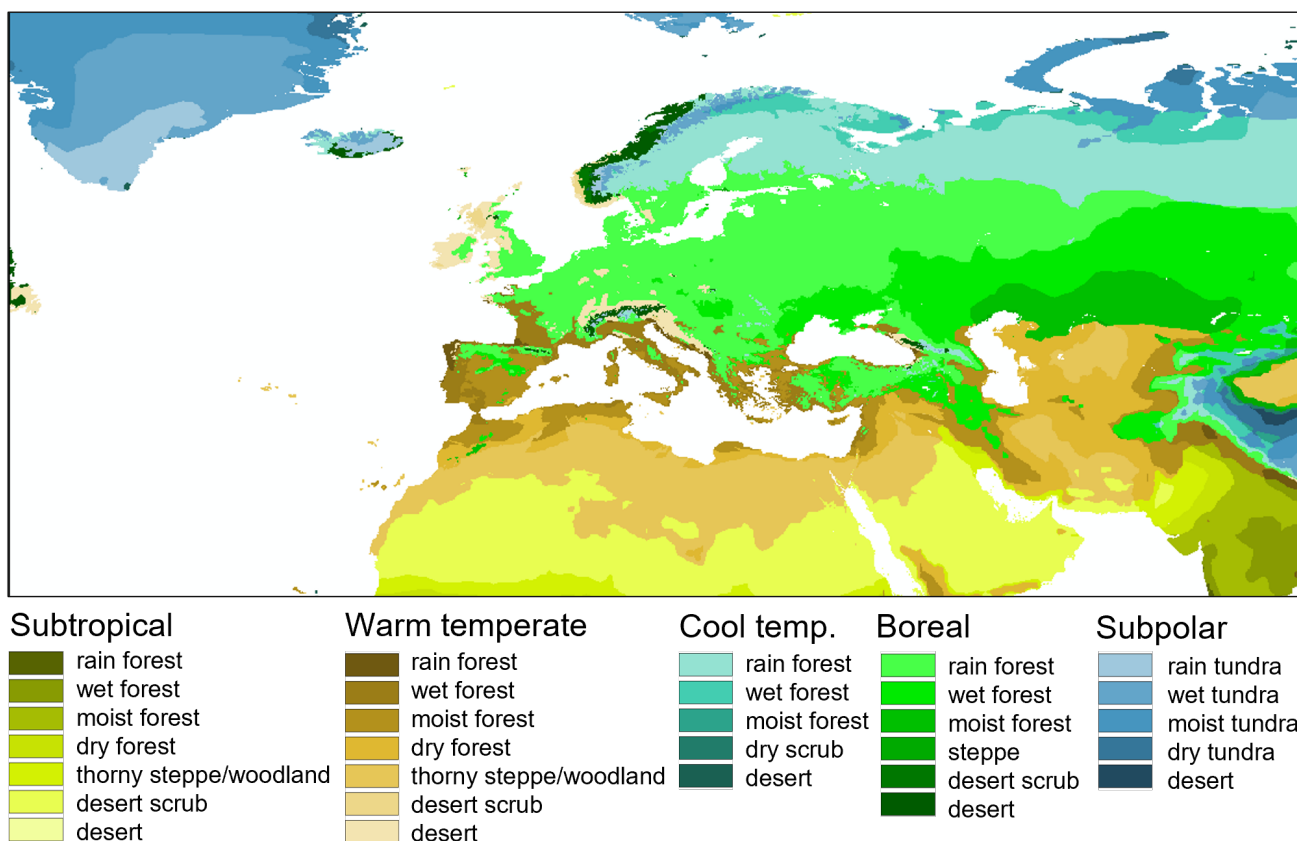


**Figure 2.** Holdridge Life Zones map for the extent of LANDMATE PFT

In the past, the HLZ concept was not only found useful for global applications but successfully implemented especially for regional mapping approaches due to its ability to capture regional climate features with the support of bioclimatic variables (Daly et al., 2003; Tatli and Dalfes, 2016). Further, the HLZ concept was used for LULC change predictions, such as land use impact assessments, related to current and future climate change scenarios (Chen et al., 2003; Skov and Svenning, 2004; Yue et al., 2006; Saad et al., 2013; Szelepcsényi et al., 2018). With the implementation of climate data through the HLZ concept, the resulting PFT maps become more detailed and can be customized to individual regions without losing global consistency.

### 2.2.5 Plant Functional Types

Table 3 shows the LANDMATE PFTs that are based on the PFTs introduced by Wilhelm et al. (2014). The implementation of an irrigated cropland PFT (PFT 14) that is currently being developed within the HICSS project LANDMATE will be implemented



in a later version of the dataset. In the initial version that is presented in this article, all cropland proportions are assigned to the cropland PFT (PFT 13).

**Table 3.** LUCAS plant functional types based on Wilhelm et al. (2014) with modified crop types.

PFTs	Names
1	Tropical broadleaf evergreen trees
2	Tropical deciduous trees
3	Temperate broadleaf evergreen trees
4	Temperate deciduous trees
5	Evergreen coniferous trees
6	Deciduous coniferous trees
7	Coniferous shrubs
8	Deciduous shrubs
9	C3 grass
10	C4 grass
11	Tundra
12	Swamp
13	Non-irrigated crops
14	<i>Irrigated crops</i> <sup>7</sup>
15	Urban
16	Bare

### 2.2.6 Potential C4 grass fraction NACP MsTMIP

The initial land cover map from the ESA-CCI LC does not provide a distinction between C3 and C4 grassland. Therefore, an additional product is used after applying the CWP. The map from the North American Carbon Program Multi-scale Synthesis and Terrestrial Model Intercomparison Project (NACP MsTMIP; Wei et al., 2014) is constructed based on the synergetic land cover product (SYNMAP) by Jung et al. (2006). SYNMAP is a combination of multiple high-resolution LULC products using a fuzzy agreement approach. The NACP MsTMIP map uses the grassland fractions from the SYNMAP product and the C4 grass distribution is estimated supported by growing season temperature based on present climate conditions (Wei et al., 2014). The map is provided in 0.5° horizontal grid resolution for the period from 1801 to 2010. For the preparation of LANDMATE PFT the NACP MsTMIP map of 2010 is used.

<sup>7</sup>the irrigated crop PFT is currently empty (see section 3.4)



### 2.3 LUCAS - land use and land cover survey

The harmonized LUCAS *in situ* land cover and use database for field surveys from 2006 to 2018 (d'Andrimont et al., 2020) is the most consistent ground truth database for the European Continent. The survey was carried out at three-yearly intervals between 2006 and 2018. The systematic sampling design of the survey consists of a theoretical, regular grid over the European Continent with ~2 km grid size. The reference point locations are the corner points of the theoretical grid. Not all locations within the survey were easily accessible. Therefore, the survey is supported by *in situ* photo interpretation, *in-office* photo interpretation and satellite data in the latest time steps 2015 and 2018 (table 4). However, the main proportion of the reference points was recorded through location visits at all time steps, which makes this land survey the most reliable and consistent ground truth database for Europe.

**Table 4.** Number and recording method of reference points in the LUCAS land cover and use database per timestep.

Year	Reference points	<i>in situ</i>	<i>in situ</i> PI <sup>8</sup>	<i>in-office</i> PI <sup>9</sup>	GT <sup>10</sup> [%]
2006	168401	155238	13163		92.18
2009	234623	175029	59594		74.6
2012	270272	243603	26669		90.13
2015	340143	242823	25254	71970	71.39
2018	337854	215120	22894	99803	63.67

The extent of the LUCAS survey was increased over time. The 2006 survey covered 11 countries while the 2018 map covers large parts of the European Continent with 28 countries. Throughout the survey, the ground truth data has been continuously checked for quality and plausibility. For the accuracy assessment of the LANDMATE PFT map the ground truth points of the year 2015 are employed (Sect. 4). In order to avoid confusion between the FPS LUCAS and the LUCAS ground truth dataset, the latter will be further referred to as **Ground Truth Survey** or **GT-SUR**.

### 3 Cross-walking procedure - ESA-CCI LC classes to PFTs

The CWP from ESA-CCI LC classes to PFTs presented in this article is based generally on (1) the translation introduced by Poulter et al. (2015) and (2) the translation by Wilhelm et al. (2014). Both translations are not just combined with each other but modified using additional data. The following sections introduce the PFTs of LANDMATE PFT aggregated into groups and give an overview of the decisions on modifications that are made during the production process based on literature and additional data. The final LANDMATE PFT map is shown in fig. 3.

<sup>8</sup>Photo interpretation close to the reference location

<sup>9</sup>Photo interpretation with supporting data, such as satellite images

<sup>10</sup>Ground truth



### 3.1 Trees and shrubs, tropical and temperate | PFT 1-8

The LANDMATE PFTs are more diversified regarding tree-PFTs than the generic ESA-CCI PFTs. The expansion of tree-PFTs to six in total was done at the expense of two shrub-PFTs. The increase of tree-PFT diversity is done in order to address the strong biogeophysical impacts of forested areas on regional and local climate, such as decreased albedo and increased roughness length (Bright et al., 2015). The effects of forested areas on near-surface climate are distinctively different to the effects of shrub or grass covered areas, and are also highly depending on tree species composition and latitudinal range (Bonan, 2008; Richardson et al., 2013). Another reason for the six tree-PFTs is the intended use of the PFT maps in RCMs. In the Land Surface Models (LSMs) of current generation RCMs, where a distinction is rather made between different tree or tree community types than between different shrub types. Therefore and with regard to the implementation process that needs to be done for each RCM individually, an increase in the number of tree-PFTs and a decrease in the number of shrub-PFTs is considered to be convenient. Accordingly, the tree and shrub proportions were distributed following both, the needleleaf and broadleaf definitions of the ESA-CCI LC classes as well as the HLZ map, where the HLZ map was decisive for an assignment of forest proportions to the temperate or tropical tree-PFT, respectively. Following a comparison with different forest datasets over Europe (not shown), the tree proportions in the translation of the mixed land cover classes (e.g. lass 61 - Tree cover, broadleaved, deciduous, closed (>40%)) are increased to be in line with the indicated overall forest amount over Europe.

### 3.2 Grassland | PFT 9 & 10

The generic ESA-CCI PFTs include a natural grassland- and a managed grassland-PFT to include grassland and cropland respectively. The LANDMATE PFTs include two grassland-PFTs, distinguishing between C3 and C4 grass. The contrasting photosynthetic pathways and therefore contrasting synthetic response to CO<sub>2</sub> and temperature determine specific ecosystem functions for both PFTs respectively. The main differences are found in global terrestrial productivity and water cycling (Lattanzi, 2010; Pau et al., 2013). The translation from the LULC classes that contain grassland proportions into C3 or C4 grass-PFTs respectively is supported by a map of potential C4 vegetation by Wei et al. (2014) where the potential global distribution of C4 is estimated using bioclimatic parameters (Sect. 2.2.6).

### 3.3 Tundra and swamps | PFT 11 & 12

The specific vegetation PFTs tundra and swamps are treated individually in LANDMATE PFT. Tundra is mostly used for the polar and subpolar HLZs, where the climatic conditions require a clear distinction of the land surface properties to the boreal and temperate regions regarding exchange and feedback processes with the atmosphere (Thompson et al., 2004). Chapin Iii et al. (2000) further suggest a differentiation of vegetation composition within these northern vegetation communities, which can also be realized using the introduced translation. The swamp-PFT is mostly used for translating the ESA-CCI LC mosaic tree/shrub/herbaceous classes and also partly for the flooded tree cover classes in most of the HLZs. Swamps occur mainly in the boreal and polar regions.



### 3.4 Cropland | PFT 13 & 14

Currently, two cropland-PFTs are defined in the LANDMATE PFT map. The cropland-PFT (PFT 13, see table 3) includes  
205 all managed, agricultural land surface proportions. The uncertainties of the translation of the ESA-CCI cropland classes and  
mixed cropland classes into the cropland-PFTs was investigated by Li et al. (2018) where the comparison of LULC change in  
the ESA-CCI PFT maps against other LULC products showed inconsistencies between global trends and geographical patterns  
between the products. However, Li et al. (2018) provide a modified CWT that was adjusted in regard to an improved knowledge  
base on how to translate LULC classes into PFTs for climate models. Particular focus is laid on mosaic classes and the sparsely  
210 vegetated classes of which appear numerous in ESA-CCI LC. Therefore, the translation from Li et al. (2018) for cropland is  
adopted into the present CWP.

The irrigated cropland-PFT (PFT 14, see table 3) is currently empty in the LANDMATE PFT map Version 1.0. This decision  
is made following intense research on available irrigation information. The ESA-CCI LC map that is used as initial input con-  
tains an "irrigated cropland" class but this information was not used in the process. The investigation on irrigated areas included  
215 the comparison of ESA-CCI LC to other products that are available, such as the irrigation map from the FAO (Siebert et al.,  
2005). Although the ESA-CCI LC quality assessment shows a very good agreement of the ESA-CCI LC irrigated cropland  
with the validation database (ESA, 2017), the comparison showed considerable differences between the products. The success  
of detection of irrigated areas is highly dependent on the correct detection of the crop types to infer the water needs of the  
respective crops, on atmospheric and environmental conditions and on the availability of multi-temporal, high resolution im-  
220 agery (Bégué et al., 2018; Karthikeyan et al., 2020). Further, most remote sensing applications depend highly on ground truth  
data and local knowledge. Applications using different satellite imagery to detect agricultural management practices, such as  
irrigation, are only successfully tested and applied in local spatial units (Rufin et al., 2019; Ottosen et al., 2019). Therefore,  
the irrigated cropland PFT remains unoccupied for now. Nevertheless, PFT 14 is defined within LANDMATE PFT Version  
1.0 for the purpose of adding irrigated LULC fractions in the future. For the long term LUCAS LUC dataset (Hoffmann et al.,  
225 submitted) which is extended backward and forward based on the LANDMATE PFT map for Europe 2015, irrigated cropland  
areas are already implemented following the irrigated area definition of the Land Use Harmonization (LUH2) dataset (Hurt  
et al., 2011).

### 3.5 Non-vegetated | PFT 15 & 16

The non vegetated-PFTs in the LANDMATE PFT dataset are urban and bare. The urban grid cells from ESA-CCI LC are  
230 directly translated into urban fractions for all HLZs in the CWP. The same applies for all bare ground proportions that are  
translated fully into the bare-PFT. In addition, the ESA-CCI LC mixed classes are split up and the bare ground proportions  
within the mixed classes are added to the bare-PFT. The explicit treatment of urban areas and especially differentiation from  
bare ground provides the possibility to resolve urban surface characteristics in RCMs. The treatment of urban areas as a slab  
surface or as an equal to rock surface as done in several RCM approaches cannot account for the complex geobiophysical



235 processes associated with an urban agglomeration (Daniel et al., 2019; Belda et al., 2018). Due to the distinction of the two  
surface types, the LANDMATE PFT map can be used for impact studies with an urban focus.

### 3.6 Water, permanent snow & ice

The LANDMATE PFTs do not include individual PFT definitions for water and snow/ice respectively. Regarding the water  
representation, most currently used RCMs are utilizing a land-sea-mask to account for oceans and inland water areas. Therefore,  
240 an explicit definition of water as individual PFT has not been implemented. Consequently, water grid cells are set to no data. In  
the present translation, the snow/ice grid cells from ESA-CCI land cover are translated into bare-PFT following Wilhelm et al.  
(2014).

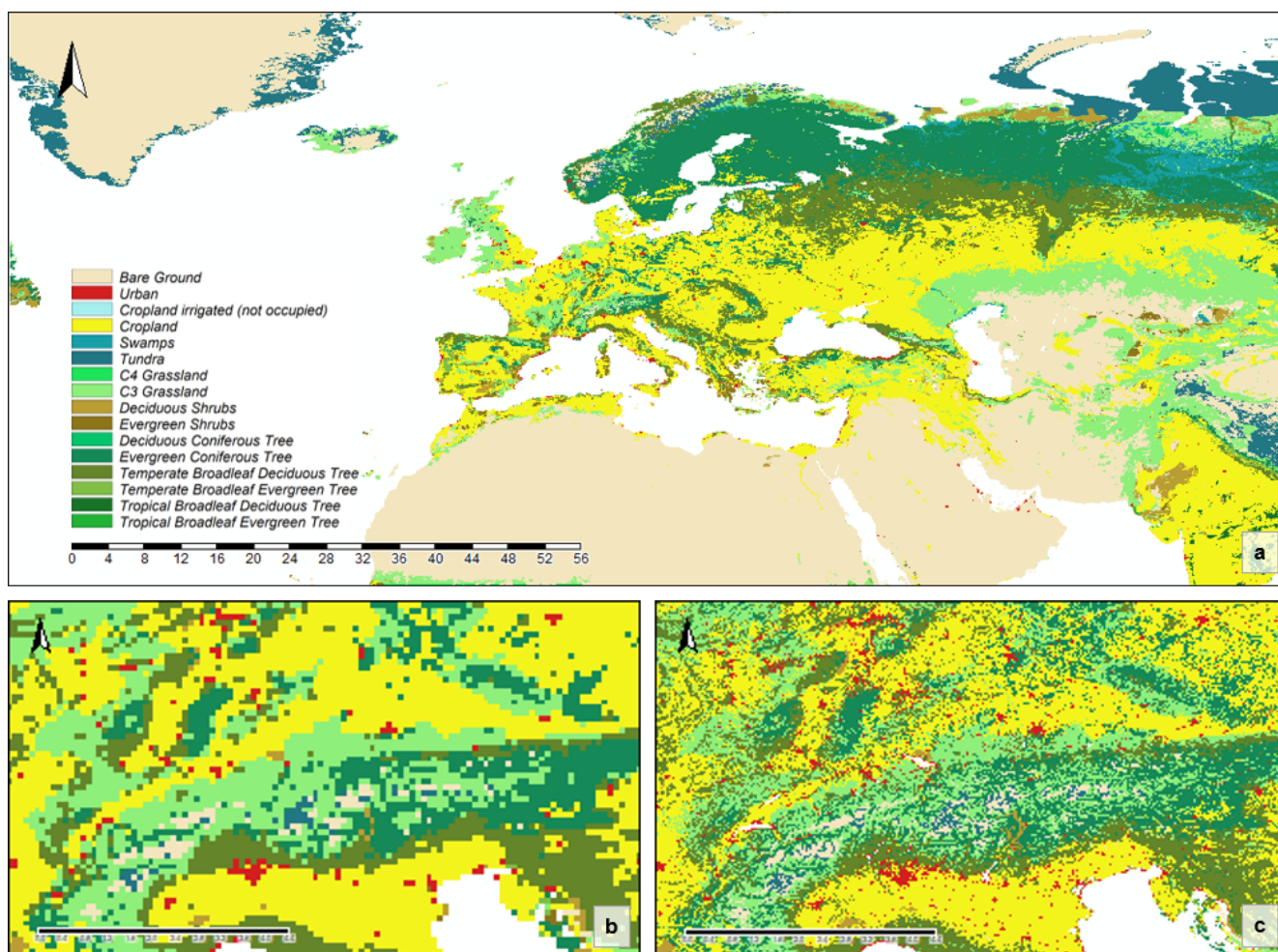


**Figure 3.** LANDMATE PFT map for Europe for 2015 (a). Below a map section of the Alpine region shows an example of the resolution  
difference between LANDMATE PFT 0.1 (b) and LANDMATE PFT 0.018 (c). LANDMATE PFT 0.018 is used in the present accuracy  
assessment. For improved visualization all maps show the majority PFT per grid cell.



#### 4 Quality assessment of the LANDMATE PFT map

The LANDMATE PFT map is based on the ESA-CCI LC map which was quality checked and compared to similar LULC products on a global (ESA, 2017; Yang et al., 2017; Hua et al., 2018; Li et al., 2018) and regional level (Reinhart et al., 2021a; Vilar et al., 2019). However, the translation from LULC classes to PFTs necessarily results in change of the map. The final product, the LANDMATE PFT map, is intended to be used in RCMs, which means the quality of the final product must be assessed in addition to the available quality assessments of the initial ESA-CCI LC map. In order to overcome the resolution difference, which is non negligible between LANDMATE PFT and the reference data GT-SUR, the LANDMATE PFT map is prepared on 0.018° horizontal resolution, which corresponds closely to the 2 km theoretical grid of GT-SUR.

The design of such a quality assessment of a large scale map product is not trivial, especially since the map product itself and the reference data are often different in structure and nomenclature, given that ground truth reference data is mostly collected as point data and independently from the assessed map product Foody (2002); Wulder et al. (2006); Olofsson et al. (2014). In order to produce reliable quality information for LANDMATE PFT, the present assessment follows closely the well established good-practice recommendations. Nevertheless, adjustments are done to account for the fractional structure of LANDMATE PFT. Section 4.2 provides additional information on the requirements of a "good practice" accuracy assessment, the key components and the selected sampling design and metrics.

##### 4.1 Research area

The coverage of GT-SUR in the year 2015 includes 28 countries which are highlighted in dark grey in fig. 4.

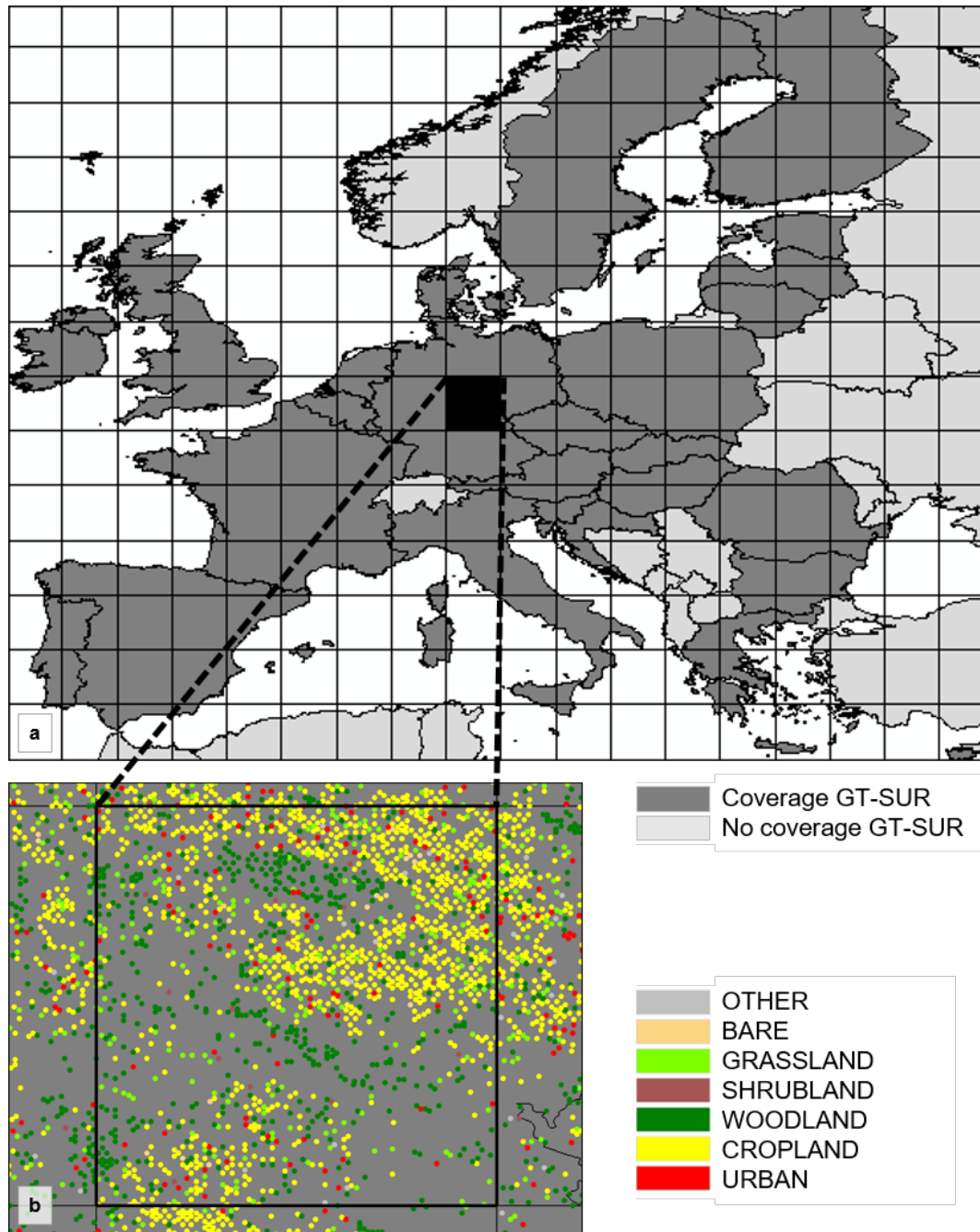


**Figure 4.** Coverage of the Land Use and Coverage Area frame Survey (LUCAS) for reference year 2015 (top). The lower figure shows the points and LULC group representation within the grid cell highlighted in black color in the top map as an example for the whole research area.



260 The total number of GT-SUR points for 2015 is 340,143. Out of these points, 338,619 points (~99.55%) are covered with  
valid LANDMATE PFT grid cells of the assessed LULC groups and can be used in the analysis. Countries located within  
the contiguous area but missing in the assessment are Switzerland, Norway, the Russian Oblast Kaliningrad, Bosnia and  
Herzegovina, Montenegro, Albania, Serbia, Kosovo, North Macedonia, and Belarus. Figure 4 also shows the 2.5° grid that was  
used for the analysis of the accuracy assessment results (Sect. 4.3). Due to the fine scale and the high number of points over the  
265 whole research area, the visualization of the spatial analyses on continental scale is challenging. Therefore, the research area is  
split up through an overlay of a 2.5° grid (as shown in fig. 4). The overall and class-wise accuracy results for all points within  
each 2.5° grid cell are aggregated in order to identify large scale spatial quality differences for the analyzed LULC groups.  
Additionally, the total number of points for each LULC group per grid cell are displayed in section 4.3.

#### 4.2 Accuracy assessment - background & design

270 The key components of the accuracy assessment of a large-scale land cover product are **objective, sampling design, response  
design** and the final **analyses and estimation** (Wulder et al., 2006). All of the key components have great impact on the  
quality of the assessment and further, on the final metrics, especially in the present assessment, where reference and assessed  
dataset differ widely in structure. LANDMATE PFT is a gridded dataset with fractional LULC classes but no information  
on the subgrid location within the grid cell. Other than that, the points of GT-SUR have fixed locations expressed through  
275 exact coordinates, but no (exact) information on the spatial extent of this class. Another challenge is the fractional structure of  
LANDMATE PFT itself, where one unit (grid cell) possibly contains multiple fractions. Therefore, the design of the accuracy  
assessment needs to be customized to the **objective**, which is to determine the overall quality of the LANDMATE PFT map for  
Europe 2015 as well as the quality of individual LULC type representation within the map in order to derive recommendations  
for the use of LANDMATE PFTs in RCMs.

280 When it comes to the **sampling design**, sampling size, spatial distribution of the respective sample and the representation  
of each LULC group or class within the sample are crucial to produce reliable quality information about a LULC product  
(Stehman, 2009). However, the collection of ground truth data is a rather expensive procedure regarding time and money, which  
needs to be considered during the process. The sample size is therefore a compromise size and cost. In the present assessment,  
an existing ground truth database containing over 340,000 records is used as reference which eliminates the possible issue of  
285 a too small sample size. It is also known that all assessed LULC groups are represented in a sufficiently high number (Table  
6). Nevertheless, the present assessment is a special case situation with every unit of LANDMATE PFT containing more than  
one LULC group potentially. Therefore, the subsets are selected through application of a filter to capture the map accuracy in  
a way that accounts for the fractional structure within the grid cells in the LANDMATE PFT map (see section 4.2.1).

The **response design** deals with the spatial support regions (SSR) and the labelling protocol or classification harmonization.  
290 The SSR is a buffer region around a sampling unit that is selected to account for small-scale landscape heterogeneity that is  
likely not captured by larger scale map products. In the present case, the sampling design is selected in a way that the grid  
cells of LANDMATE PFT serve as SSR for each GT-SUR point. A fraction is not located precisely at one location within  
the respective grid cell but evenly distributed over the whole grid cell. Assuming, the uniformly distributed fraction can occur



in small patches or in one large patch within the grid cell, the whole grid cell is defined as SSR for the respective LULC  
295 group. The labelling protocol needs to be determined to deal with the different legends of the reference and the assessed map.  
The harmonization of legends is selected in regard to the objective of the respective assessment, as in this case, to provide  
information about the quality of representation of the most dominant LULC types in LANDMATE PFT. The labelling protocol  
used in the present assessment is summarized in table 5.

The **analyses and estimation** used are error matrices, that give an overview of the overall and LULC group-wise accuracy of  
300 the LANDMATE PFT map. For both resolutions of LANDMATE PFT, the error matrices and the resulting accuracy measures  
overall accuracy (OA), producer's accuracy (PA) and user's accuracy (UA) are calculated, where PA and OA are calculated  
group-wise. The error matrix is a cross-tabulation between map and reference of the size  $q \times q$ , where  $q$  stands for the number  
of land cover classes or groups. The map classes are placed in the rows and the reference classes in the columns so that  
the diagonal of the matrix gives the sum of the correctly classified map units. The off-diagonal cell values represent the  
305 disagreement between the map and the reference. The overall accuracy is calculated according to equation 1:

$$OA = \frac{\sum_{i=1}^q n_{ii}}{n} * 100 \quad (1)$$

The sum of the agreeing diagonal elements  $n_{ii}$  of all LULC groups is divided by the number of all observations  $n$ . The  
PA represents the accuracy from the view of the map producer. The PA stands for the probability, that a LULC feature in the  
reference is classified as the respective feature by the map. The PA is calculated using equation 2 where the number of correctly  
310 classified units per LULC group  $n_{ii}$  is divided by the total number of LULC group occurrences of the reference  $n_{+i}$ :

$$PA_i = \frac{n_{ii}}{n_{+i}} * 100 \quad (2)$$

While the PA gives the proportion of features in the reference that are actually represented as those in the produced map,  
the UA is the accuracy from the perspective of the map user. It is the probability of a feature classified as such in the map is  
actually present in the reference. The UA is calculated using equation 3, where the number of correctly classified pixels  $n_{ii}$  per  
315 LULC group is divided by the row sum  $n_{i+} = \sum_{j=1}^p n_{ji}$ :

$$UA_i = \frac{n_{ii}}{n_{i+}} * 100 \quad (3)$$

#### 4.2.1 Dataset harmonization & filter

The quality assessment is done assigning the PFT type with the maximum fraction per grid cell to the GT-SUR points located  
within respective grid cell. The classifications of both datasets need to be harmonized in order to make the comparison as  
320 detailed as possible but also to be able to produce reliable and robust results for the RCM community. For the analysis, the  
classifications of LANDMATE PFT and the GT-SUR are harmonized as shown in table 5.



**Table 5.** Classification harmonization between LANDMATE PFT map and GT-SUR

GT-SUR LC group	GT-SUR group name	LANDMATE PFT number	LANDMATE PFT name	Harmonization group number	Harmonization name
A	Artificial Land	15	Urban	1	URBAN
B	Cropland	13 14	Non-irrigated Crops Irrigated crops	2	CROPLAND
C	Woodland	1 2 3 4 5 6	Tropical broadleaf evergreen trees Tropical deciduous trees Temperate broadleaf evergreen trees Temperate deciduous trees Evergreen coniferous trees Evergreen deciduous trees	3	WOODLAND
D	Shrubland	7 8	Coniferous shrubs Deciduous shrubs	4	SHRUBLAND
E	Grassland	9 10	C3 Grass C4 Grass	5	GRASSLAND
F	Bare land	16	Bare	6	BARE AREAS
G	Water	11	Tundra	7	OTHER
H	Wetlands	12	Swamps		
Other	Marine areas				

The LULC groups URBAN, CROPLAND, WOODLAND, SHRUBLAND, GRASSLAND, and BARE AREAS are harmonized without applying modifications to the classifications. The LANDMATE PFTs can easily be grouped or directly adopted while the GT-SUR level one classification (letters A-H) is completely adopted into the harmonized groups. The LANDMATE PFT map is a product developed for the use in RCMs. In general, RCMs implement a land-sea-mask to determine aquatic areas for both, inland and marine water. Therefore, the categories WATER and MARINE areas are neglected in the analyses. The LANDMATE PFTs "Tundra" and "Swamp" can not be assigned with a sufficient agreement to the GT-SUR class definitions. Therefore, the GT-SUR groups water, wetlands and marine areas as well as the LANDMATE PFTs Tundra and Swamps are merged into the group "OTHER" for the assessment. Although the group cannot be evaluated regarding the quality of the



330 LANDMATE PFT map, the group needs to be involved in the assessment to keep the numbers in the assessment correct and reliable for all other groups.

Both datasets are provided in a regular Gaussian grid (WGS84 EPSG:4326) so that no reprojection of the datasets needs to be done for the comparison. The descriptive statistics for each LULC group for the reference GT-SUR and the LANDMATE PFT dataset are summarized in table 6.

**Table 6.** General information on data in the comparison

LULC group <sup>11</sup>	GT-SUR <sup>12</sup>	LANDMATE PFT 0.018 <sup>o13</sup>	Dominant LANDMATE PFT 0.018 <sup>o14</sup>
URBAN	14,393	65,000	7,577
CROPLAND	83,295	248,301	136,970
WOODLAND	124,374	277,290	124,437
SHRUBLAND	27,298	302,035	19,790
GRASSLAND	66,541	333,948	44,244
BARE AREAS	10,395	31,756	4,148
OTHER	12,340	28,823	1,470
Sums	338,636		338,636

335 The LANDMATE PFT dataset includes multiple LULC fractions per grid cell. Accordingly, the area proportion of the dominant LULC group varies widely and thus the likelihood that the GT-SUR point sample falls within this area. The filter applied is categorizing the grid cells regarding the proportion of the dominant LULC group, the higher the threshold, the stricter the filter and the more likely a specific sample falls into the subgrid fraction of the dominant class. The filter set numbers 1-10 are representing the cells containing a minimum of 10 - 100% of the dominant LULC group according to table 7.

<sup>11</sup>LULC group analyzed in the quality assessment

<sup>12</sup>GT-SUR points assigned per LULC group

<sup>13</sup>number of grid cells in LANDMATE PFT that have a share of the respective LULC group >0%

<sup>14</sup>Sum of LANDMATE PFT grid cells where the respective LULC group is represented dominantly



**Table 7.** Filter sets with varying dominant LULC group share per grid cell from >10% to 100%

Filter set number	fraction size of dominant LULC group	LANDMATE PFT cells within filter set
1	>10 %	338619
2	>20 %	338619
3	>30 %	336703
4	>40 %	311238
5	>50 %	259073
6	>60 %	203343
7	>70 %	137412
8	>80 %	74765
9	>90 %	26993
10	100 %	1449

### 340 4.3 Results

In order to show the impact of the applied spatial filter, the spatial distribution of agreement and disagreement of LANDMATE PFT with the reference GT-SUR is investigated. The point counts and percentage agreement are aggregated and averaged, respectively, per 2.5° grid cell. After giving an overview over the overall accuracy measures the individual LULC group results are discussed in the following subsections. Note that due to the low overall point count as shown in table 6, the LULC groups  
 345 SHRUBLAND and BARE AREAS are discussed together in section 4.3.5. Figure 5 shows the spatial distribution of the filter sets over Europe while fig. 6 shows the overall accuracy for the filter sets.

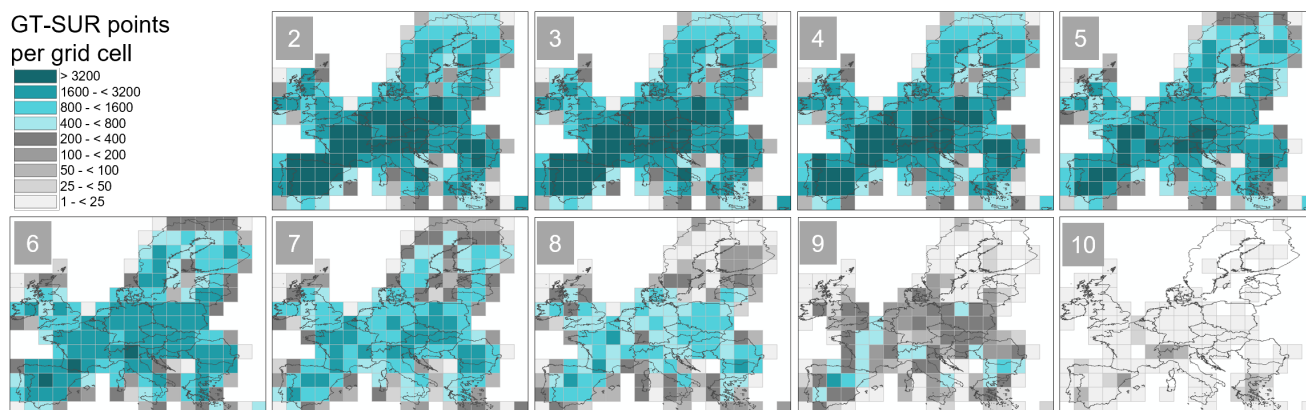


**Figure 5.** The distribution of the varying dominant LULC group filter sets over the research area in Europe. Since the >10% and the >20% filter set share the same number of points the >10% filter set is not shown.

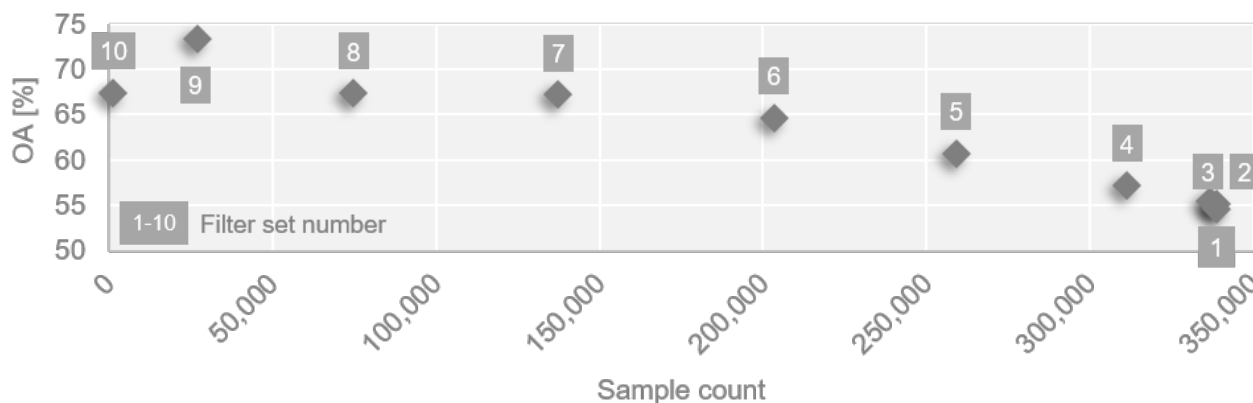


**Figure 6.** Overall accuracy for the full domain of the 10 filter sets as introduced in table 7 as function of filter set size. Filter set numbers are shown in grey boxes.

In order to be able to capture the LULC group diversity and distribution characteristics of LANDMATE PFT, the filter set must be distributed well over the respective area and contain a sufficiently large proportion of the total cells. Figure 5 shows that the filter sets are distributed reasonably well up to filter set 7. Filter set 8 shows a quite patchy pattern and a strongly decreasing sample number in Northern Europe. Within filter set 9, the patchy pattern of low sample count per 2.5° grid cell spreads over the whole continent. While filter set 9 could still be used for evaluation of LANDMATE PFT for limited regions in Europe, filter set 10 is clearly not evaluable due to the overall small sample count (< 1500). This pattern is also found for filter sets 9 & 10 of the individual LULC groups. The filter set sizes as well as the applied filter itself have direct impact on the OA shown in fig. 6. The decreasing OA towards the higher sample count is an effect of the LANDMATE PFT grid cell heterogeneity representation in each filter set. Filter set 1-3 include all LANDMATE PFT grid cells where the dominant LULC group occupies a minimum of 10% to 30% respectively. Therefore, the probability that the GT-SUR point sample within the respective grid cell represents a location that is occupied by one of the non-dominant LULC groups is relatively high. The applied filter accounts for the impact of the structure difference of the two datasets. The higher probability of agreement is reflected in the increasing OA for the samples that include only grid cells with an occupation of 50% or more of the dominant LULC group. Sample 9 & 10 represent the LANDMATE PFT dataset not adequately regarding distribution and diversity while sample 8 shows a poor coverage in northern Europe. In order to include the largest proportion of the total sample in the analysis, the point count per LULC group as well as the PA per 2.5° grid cell for filter set 2 is analyzed in the results section (fig. 7). In order to give an overview of the spatial accuracy for the evaluable filter range, The respective figures for filter set 5 and 7 are shown in Appendix B (tables B1 & B2).

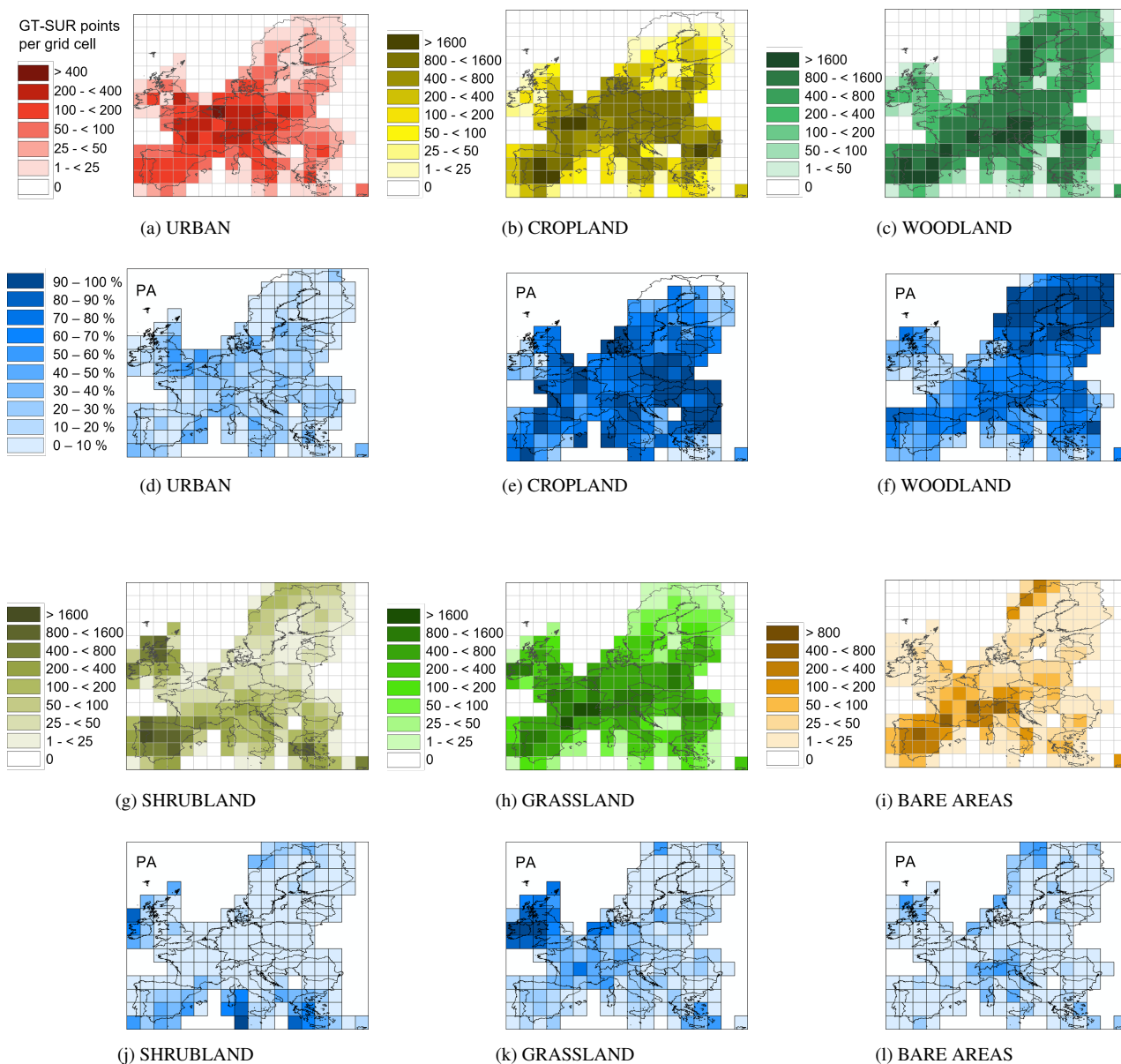


**Figure 7.** Total count of GT-SUR points per 2.5° grid cell (a-c; g-i) and producer's accuracy for the individual LULC groups (d-f;j-l) for filter set 2 (dominant LULC group occupies > 20% per LANDMATE PFT grid cell)

### 365 4.3.1 URBAN

The urban representation in LANDMATE PFT for filter set 2 is shown in fig. 7a and 7d. The PA for the filter sets 1-10 is shown in fig. 8 where an overall low PA for all filter sets is found. With increasing proportion of the dominant LULC group URBAN



the PA increases slightly but is still lower than 40% for samples that include enough points to be considered representative for the research area. The overall low PA is reflected in the URBAN maps in fig. 7 as well as in fig. B1 and B2.

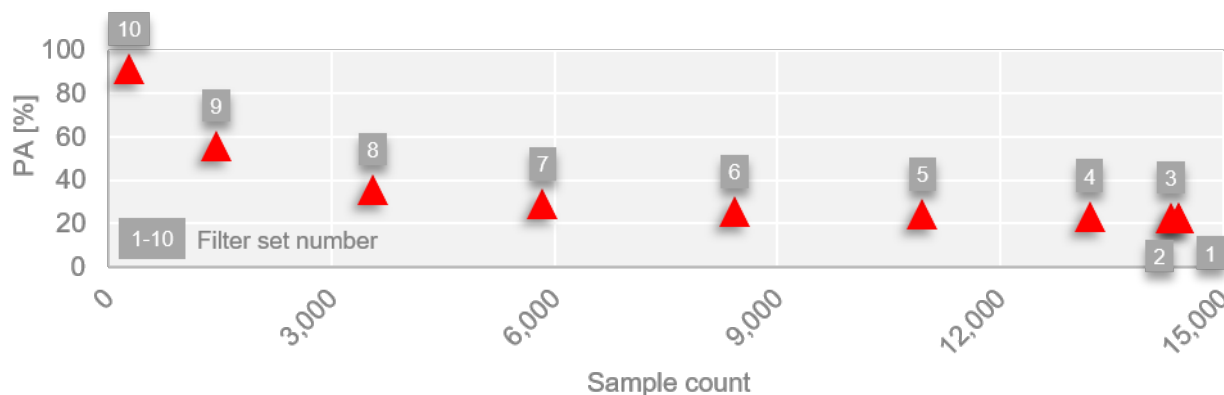


**Figure 8.** Producer's accuracy of the 10 filter sets (Filter set numbers in grey boxes) for the LULC group URBAN as a function of sample count per filter set.

370 A visual check of the map agreement between LANDAMTE PFT and GT-SUR revealed the issue that leads to the overall low PA. Figure 9 shows four large URBAN agglomerations in different areas of Europe where the red points represent GT-SUR urban points while the white points represent GT-SUR point representing non-urban LULC groups. The grey-scaled squares represent the LANDMATE PFT URBAN fractions from zero (no coverage, white) to one (full coverage, black) within one grid cell.

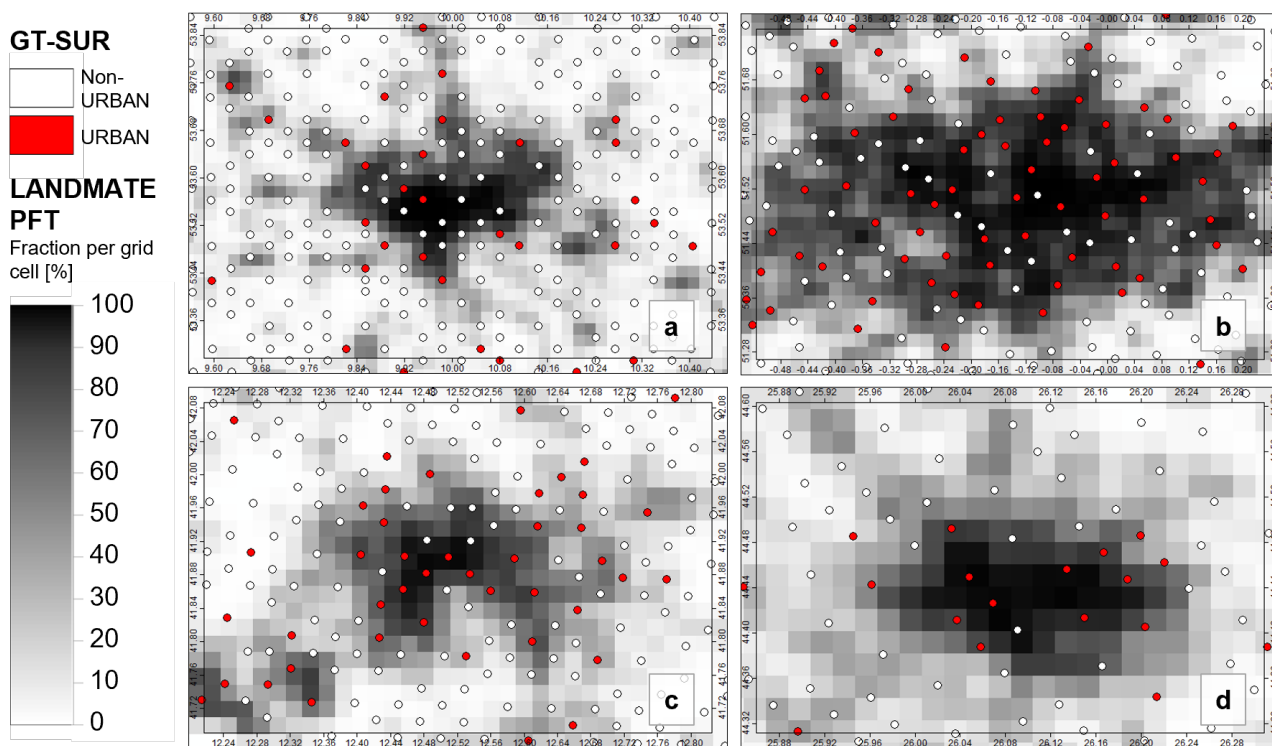


**Figure 9.** Examples of URBAN representation in LANDMATE PFT (greyscale grid) and GT-SUR (points). Cities shown are Hamburg (a), London (b), Rome (c) and Bukarest (d).

375 The LANDMATE PFT grid cells with a large urban fraction indicate the respective city core while the GT-SUR points that  
are located within the city core are mostly not classified as URBAN. However, the GT-SUR points do not fail to represent the  
structure of urban areas because they are characterized through a heterogeneous pattern of sealed surfaces, recreational areas  
(e.g. parks) and different building types and density, not through a homogeneous sealed area. The LANDMATE PFT map  
represents this heterogeneous structure through the varying fractions of non-urban PFTs within the grid cell. However, in order  
380 to make the impact of a larger city visible in an RCM simulation, it is beneficial for LANDMATE PFT to represent a larger city  
with a dense core structure. In order to verify the representation of the large URBAN agglomerations in Europe, a comparison  
with the World Settlement Footprint for 2015 (WSF, Marconcini et al., 2020) dataset was done (not shown). The comparison  
showed that not only larger agglomerations but also smaller patches of settlements are represented well in LANDMATE PFT.  
Therefore, despite the low agreement with GT-SUR in the present assessment, the URBAN PFT of LANDMATE PFT 2015 is  
385 of sufficiently good quality and suitable to represent urban land cover in high resolution (~2 km) RCM simulations. Due to the  
abovementioned comparability issues the UA of the LULC group URBAN will not be further discussed.



### 4.3.2 CROPLAND

The CROPLAND representation in LANDMATE PFT shows, together with WOODLAND the highest PA for the research area. As shown in fig. 10 the PA for all filter sets is > 80% which is to be considered as a very good agreement with the reference.  
390 reference.

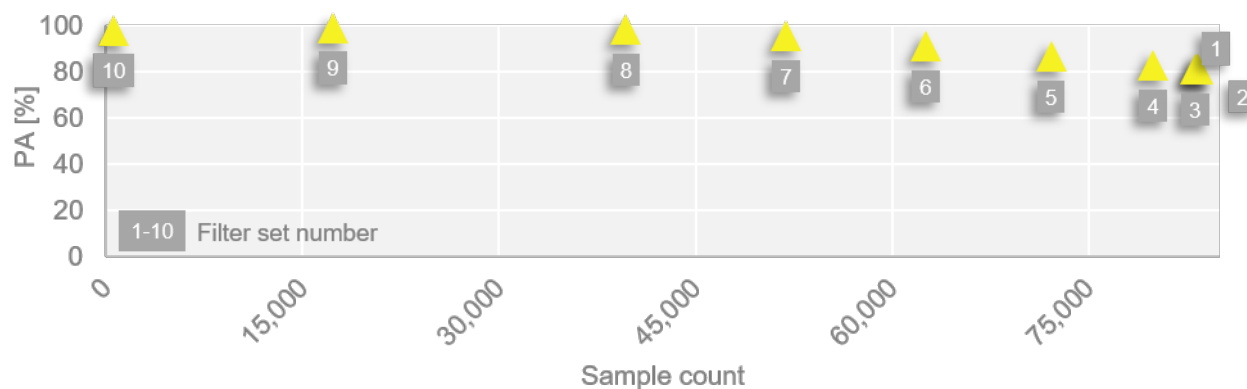


**Figure 10.** Producer's accuracy of the 10 filter sets (Filter set numbers in grey boxes) for the LULC group CROPLAND as a function of sample count per filter set.

Figure 7b shows the distribution of CROPLAND points in GT-SUR over the research area. CROPLAND points are the second most frequent LULC group in GT-SUR and are mainly distributed over middle and southern Europe. Although the northern European grid cells show a lower count of CROPLAND points, figure 7e shows that the PA is still very high in these areas. The PA increases with increasing filter set homogeneity (Fig. B1 and B2). Regarding the UA for CROPLAND,  
395 LANDMATE PFT shows a strong overestimation, where ~51% of the LANDMATE PFT CROPLAND cells in filter set 2 are actually another LULC group in the reference. More than half of the LANDMATE PFT CROPLAND areas are mostly WOODLAND, GRASSLAND, and a mix of the other LULC groups in the reference. The UA for CROPLAND increases rapidly towards the more homogeneous filter sets (~61% for filter set 7). However, the confusion with WOODLAND and GRASSLAND is non-negligible and will be discussed in section 6.

### 400 4.3.3 WOODLAND

For the representation of WOODLAND, the PA shows the second highest values with > 70% for all filter sets with a reasonably high point count (filter sets 1-7, fig. 11). Similar to CROPLAND, the sampling filter does not have a large impact on PA. The highest PA is reached over the northern European regions (Fig. 7f). Deficits are visible over the southern British Isles, some parts of France and the coastline along Belgium and the Netherlands. Further, the Mediterranean Coast shows a low PA within  
405 grid cells that have an overall small point count (Fig. 7c).

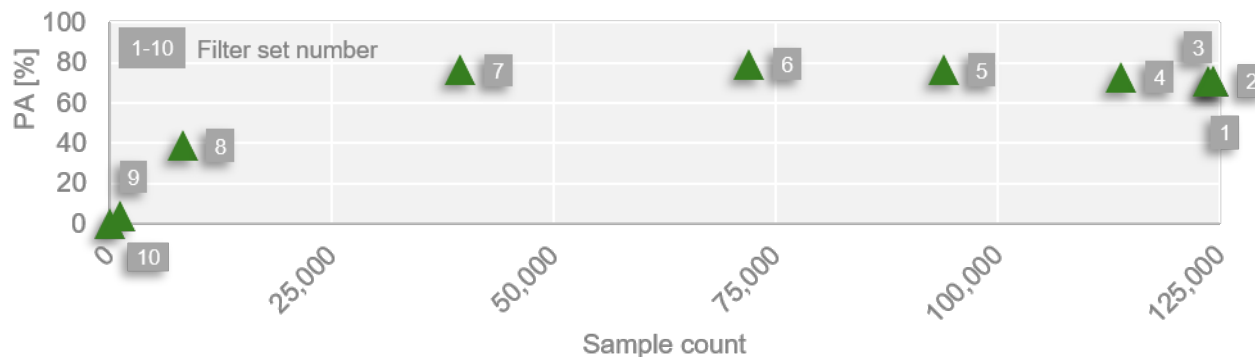


**Figure 11.** Producer's accuracy of the 10 filter sets (Filter set numbers in grey boxes) for the LULC group WOODLAND as a function of sample count per filter set.

The differences between northern and southern regions tends to increase towards the more homogeneous filter sets as shown in figures B1f and B2f. Agreement over the northern regions increases while agreement over the Iberian Peninsula decreases together with a rapid decrease of the filter set count within the corresponding grid cells. The UA for WOODLAND is noticeably higher than for all other LULC groups (> 70% for filter set 2 and increasing towards the more homogeneous filter sets) which emphasises the very good quality of WOODLAND representation in LANDMATE PFT. (~10% for filter set 2). Further, ~4% of the total LANDMATE PFT cells representing WOODLAND are actually CROPLAND or OTHER.

#### 4.3.4 GRASSLAND

The GT-SUR sampling points show the highest GRASSLAND coverage in central Europe with the highest occurrence in Ireland and the southern part of France (Fig. 7h). The PA for LANDMATE PFT GRASSLAND according to fig. 7k is not noticeably higher in these areas but overall highest in the Southwest of the British Isles. For all filter sets, the PA ranges between 32 and 34% which is considerably low (Fig. 12).

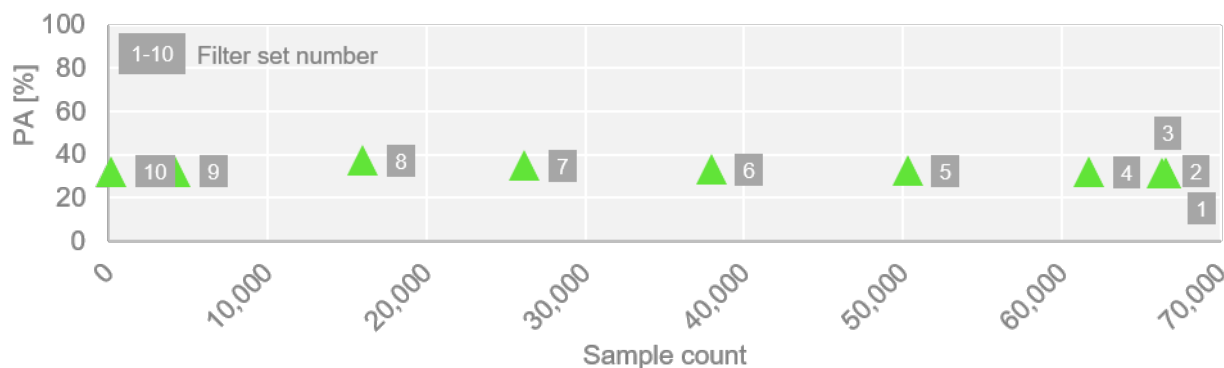


**Figure 12.** Producer's accuracy of the 10 filter sets (Filter set numbers in grey boxes) for the LULC group GRASSLAND as a function of sample count per filter set.

One reason for this low accuracy of LANDMATE PFT regarding GRASSLAND can be found looking at the results of sections 4.3.2 and 4.3.3. The UAs of CROPLAND and WOODLAND reveal that ~20% of the LANDMATE PFT CROPLAND cells and ~10% of the LANDMATE PFT WOODLAND cells are actually representing GRASSLAND in the reference, which adds up to over 60% of the total GT-SUR GRASSLAND points. Another reason is found in the dataset structure of LANDMATE PFT. A considerable amount of GRASSLAND is not part of the assessment because GRASSLAND does not make the dominant but the second dominant PFT in many grid cells (~45% of all LANDMATE PFT grid cells). Therefore, the seemingly weak GRASSLAND representation in LANDMATE PFT rather shows a weakness of the present assessment that is caused by the different dataset structures.

#### 4.3.5 SHRUBLAND & BARE AREAS

The PA for SHRUBLAND and BARE AREAS is the lowest of all assessed LULC groups with < 20% for all filter sets of both LULC groups respectively (Fig. 13 and 14). The low point count of both LULC groups might be one reason for the low PA. However, looking at the distribution of the SHRUBLAND and BARE AREA points in fig. 7i, LANDMATE PFT is not able to capture the LULC groups even in grid cells with a relatively high point count. The GT-SUR shows ~27,000 SHRUBLAND points while LANDMATE PFT shows only ~19,000. Therefore, one reason for the poor SHRUBLAND representation lies within the base map (ESA-CCI LC) used for the creation of LANDMATE PFT, where the known small count of SHRUBLAND proportions was inherited by LANDMATE PFT. It must be noted, that a large proportion of SHRUBLAND in ESA-CCI LC is part of the mixed LC classes, such as Shrubland/Cropland or Shrubland/Forest. The known deficit was partly compensated by the translation into the PFTs, where SHRUBLAND proportions were added to the total as proportions of the mixed ESA-CCI LC classes. Further SHRUBLAND makes the second dominant PFT in ~20% of the total LANDMATE PFT grid cells in the assessment. Just like for GRASSLAND, these SHRUBLAND proportions can not be addressed within the present assessment.

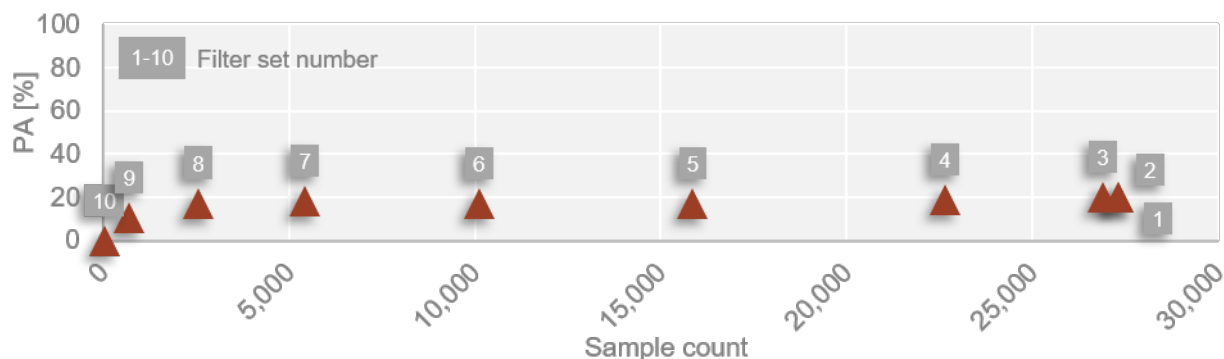


**Figure 13.** Producer's accuracy of the 10 filter sets (Filter set numbers in grey boxes) for the LULC group SHRUBLAND as a function of sample count per filter set.

The overall BARE AREAS sample count in LANDMATE PFT in filter set 2 is < 50% of the actual BARE AREA points in GT-SUR. Almost half of the GT-SUR BARE AREAS points are identified as CROPLAND while ~30% are identified as WOODLAND or GRASSLAND. Only ~17% (< 2,000 points for filter set 2) of the GT-SUR BARE AREAS are actually identified by LANDMATE PFT with the largest agreement in the Alps, Northern Great Britain, and Northern Scandinavia (Fig. 7). However, due to the comparably low sample count the spatial assessment is not robust. Just like for SHRUBLAND, the homogeneity of LANDMATE PFT cells does not have a large impact on the PA. UA is higher than PA with ~43% and increasing towards the more homogeneous filter sets. However, considering the rapidly decreasing sample count for the more homogeneous filter sets, the accuracy measures are becoming even less representative for the BARE AREA representation in LANDMATE PFT. Nevertheless, the confusion with the other LULC groups is further discussed in section 6.

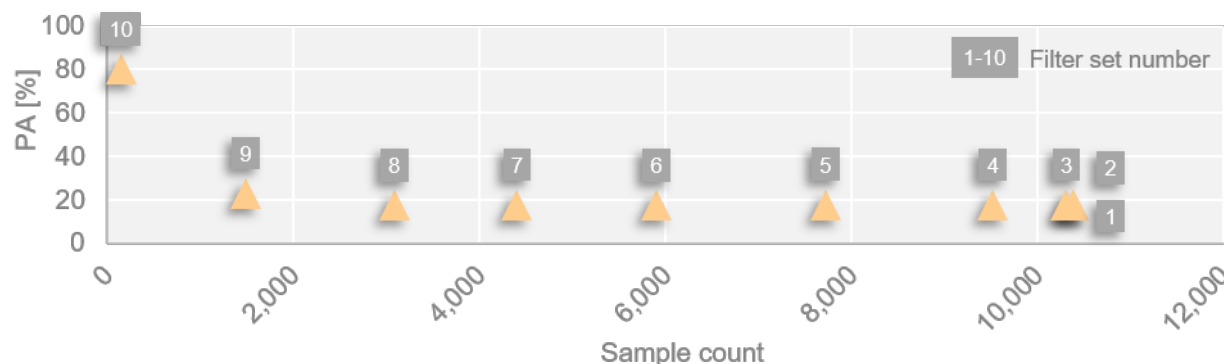


**Figure 14.** Producer's accuracy of the 10 filter sets (Filter set numbers in grey boxes) for the LULC group BARE AREAS as a function of sample count per filter set.



## 5 Data availability

The LANDMATE PFT dataset for Europe 2015 is published with the Long Term Archiving Service (LTA) for large research datasets, which are relevant for climate or earth system research, of the German Climate Computing Service (DKRZ). As World Data Center for Climate (WDCC), the DKRZ LTA is accredited as regular member of the World Data System. The LANDMATE PFT dataset for Europe 2015 is available within the LANDMATE project data at [https://cera-www.dkrz.de/WDCC/ui/ceraresearch/entry?acronym=LM\\_PFT\\_LandCov\\_EUR2015\\_v1.0](https://cera-www.dkrz.de/WDCC/ui/ceraresearch/entry?acronym=LM_PFT_LandCov_EUR2015_v1.0) (Reinhart et al., 2021b). Within the LANDMATE project, a short documentation summarizes the technical information corresponding to LANDMATE PFT.

## 6 Discussion & conclusion

The present work introduces the preparation of the LANDMATE PFT map for the European Continent based on several LULC datasets and climate data.

The LANDMATE PFT Version 1.0 is prepared in order to provide realistic, high-resolution LULC representation for RCMs. The dataset includes LULC information from different, validated sources as well as regional climate information through involvement of the HLZs. For each ESA-CCI land cover class, an individual CWT is developed to translate the original LULC classes into PFTs. The various mixed LULC classes included in the base map ESA-CCI LC are extremely difficult to resolve within RCMs. Through the developed CWP, the mixed LULC classes can be disaggregated into PFT fractions, which improves the realistic representation of these classes in RCMs. The involvement of the climate data further allows a customized translation of LULC classes for individual regions. The 16 LANDMATE PFTs are selected to provide simple transferability into various RCM families in order to be able to conduct coordinated RCM experiments where the implementation of a common, high quality LULC map provides minimum uncertainty for a multi-model ensemble.

The accuracy assessment of LANDMATE PFT is conducted in the form of a comparison with the ground truth dataset GT-SUR. In order to account for the different structure of the reference GT-SUR and the assessed LANDMATE PFT map and further the fractional structure of the LANDMATE PFT grid cells, a filter is applied. All filtered LANDMATE PFT subsets are analyzed in terms of agreement with the reference (i.e., GT-SUR). In order to investigate regional differences in accuracy measures, a spatial analysis supported by gridded maps of the research area is done. The quality of the LANDMATE PFT map is assessed using the overall accuracy (OA) and the producer's and user's accuracy (PA and UA) for the individual LULC groups. Overall, the assessment serves as recommendation and uncertainty information for regional climate modellers that use LANDMATE PFT, or the time series LUCAS LUC (Hoffmann et al., submitted), which is based on LANDMATE PFT, in RCMs.

Within the accuracy assessment, the OA does not change considerably between the evaluable filter sets of the respective LULC groups which shows that the dataset structure has no noticeable impact on that accuracy measure. The highest PA is found for CROPLAND and WOODLAND which are the dominant LULC groups in the research area. The lowest PA is found for SHRUBLAND and BARE AREAS, which are also the LULC groups with the lowest overall sample count. The UA is found to be highest for WOODLAND, followed by CROPLAND, GRASSLAND and BARE AREAS. Both accuracy measures, PA



and UA are highly influenced by the proportion of the dominant LULC group in the individual grid cell. The difference between  
480 the filter sets for UA of the LULC groups is 10 to 20% per group while the difference for PA is noticeable but considerably  
lower, which means that the applied filter has a higher influence on the former.

The URBAN representation in LANDMATE PFT represents a special case in the present assessment due to the heteroge-  
neous structure of urban areas. Both datasets, GT-SUR and LANDMATE PFT are able to represent the LULC group URBAN  
very well for their respective purpose. Nevertheless, the PA for URBAN reflects the limitations of the present assessment  
485 method. The fine scale point data of GT-SUR represents the patchwork structure of recreational areas, building blocks, and  
other urban elements at the location of the respective points while LANDMATE PFT represents the urban area as an agglom-  
eration of grid cells with URBAN as the dominant LULC group. The additional comparison with a high resolution dataset  
(WSF2015) showed that not only large but also small agglomerations of urban areas are represented well in LANDMATE PFT.  
Therefore and despite of the accuracy assessment results for the LULC group URBAN, the LANDMATE PFT dataset can be  
490 recommended to be used in RCMs that resolve urban features over the European Continent.

A limitation of LANDMATE PFT is the overestimation of CROPLAND to the expense of WOODLAND and GRASSLAND  
and the overestimation of WOODLAND to the expense of mostly GRASSLAND. This overestimation has a minor impact on  
the overall WOODLAND and CROPLAND representation but a major impact on the representation of GRASSLAND in  
LANDMATE PFT. The representation of GRASSLAND is comparably low due to the aforementioned reasons. Further, the  
495 LULC groups with the lowest point counts SHRUBLAND and BARE AREAS are not well represented, which happens due to  
the low overall sample size but also due to the overall too low representation in LANDMATE PFT, which is partly inherited  
from the base map ESA-CCI LC. The representation of these LULC groups needs to be considered when using LANDMATE  
PFT in RCM simulations using the supporting maps in fig. 7, B1 and B2.

The representation of LULC groups in LANDMATE PFT is assessed through the comparison with ground truth data. The  
500 structural differences of the datasets, where gridded data is compared to point data, is a major weakness of this assessment.  
Although the fractional structure does not have a major influence on the OA, the LULC group-wise PA and even more the UA  
is affected.

The present assessment takes into account the dominant LULC group per grid cell of LANDMATE PFT. Depending on  
the proportion of this LULC group, the second or third-most represented LULC group can occupy a considerable area of  
505 the respective grid cell. Therefore, a follow up assessment, where these LULC group proportions are also considered and  
compared to the ground truth is needed in order to investigate, if the PA of the less dominant LULC groups GRASSLAND,  
SHRUBLAND, and BARE AREAS is increased. The use of additional LULC data, like it was done for URBAN in this  
assessment, would be an additional useful step to validate the quality of GRASSLAND, SHRUBLAND and BARE AREAS  
representation in LANDMATE PFT.

510 The results show that the LANDMATE PFT map is able to represent LULC over large parts of Europe in a sufficient  
quality. Especially the dominant LULC groups are represented overall well which is highly beneficial for RCM experiments  
that require realistic, high-resolution LULC representation. Nevertheless, there are uncertainties found for the less represented  
LULC groups. When using LANDMATE PFT in an RCM it is crucial to consider these uncertainties when interpreting simu-



515 lation results. Especially the spatial distribution of uncertainties in LANDMATE PFT needs to be considered when comparing simulation results to observations because the input parameters in the employed land-surface schemes are influenced by the individual LULC, which subsequently considerably impacts on lower-atmosphere processes, such as the intensity of heat and moisture exchange. Thus, by carefully considering the issue of uncertainty introduced by the LULC input, misconclusions about RCM model performance and about small-scale interconnections can be avoided (Ge et al., 2007; Sertel et al., 2010; Santos-Alamillos et al., 2015; Reinhart et al., 2021a).

520 Beside the quality of the LULC product, the implementation process of each individual RCM is crucial for the realistic representation of LULC in regional climate model experiments. When translating a LULC product into the model specific LULC classes and structure, modifications are done that can change the map characteristics. When the LANDMATE PFT product is used in an RCM that only uses the dominant LULC fraction per grid cell, the overall LULC proportions can change. The same applies when LANDMATE PFT is used in a model with limited fractions per grid cell or a different classification  
525 system. The present assessment gives a guideline on the quality of LANDMATE PFT (Version 1.0) when used unaltered. Through the involvement of the ground truth data, regional deficits of LANDMATE PFT are presented that can be compensated during the implementation process into the individual RCM or RCM family.

The findings of the present assessment support the identification of uncertainties within the LANDMATE PFT map for Europe. Nevertheless, user feedback is crucial for the future overall improvement of LANDMATE PFT. The RCM community  
530 within the WCRP FPS LUCAS is already participating in the feedback process where implementation of LANDMATE PFT and the LUCAS LUC time series into different RCMs is comprehensively documented. The future work on LANDMATE PFT also includes the extension of the dataset to other CORDEX regions. Although, the dataset is based on various globally available datasets and therefore, can be created globally, the introduced quality assessment method must be performed for each region individually, desirably using region-specific expert knowledge. Further, the assessment should be expanded in order to  
535 include the second or third-most represented LULC group per grid cell to possibly achieve more accurate quality information about LANDMATE PFT.



## Appendix A

**Table A1.** Cross-walking table for ESA-CCI LC class 10 - Cropland, rainfed and LC class 11 -Cropland, herbaceous cover. For LC class 10 and 11, no HLZ were assigned

	1	2	3	4	5	6	7	8	9	10	11	12	13	14	15	16
<b>Tree</b>							<b>Shrub</b>		<b>Grass</b>		<b>Special vegetation</b>		<b>Crops</b>		<b>Non-vegetated</b>	
<b>Holdridge Life Zone</b>	tropical broadleaf evergreen	tropical broadleaf deciduous	temperate broadleaf evergreen	temperate broadleaf deciduous	evergreen coniferous	deciduous coniferous	evergreen	deciduous	C3	C4	Tundra	Swamps	crops		urban	bare ground
1-30										10						90

**Table A2.** Cross-walking table for ESA-CCI LC class 12 - Cropland, tree or shrub cover. For LC class 12, no HLZ were assigned

	1	2	3	4	5	6	7	8	9	10	11	12	13	14	15	16
<b>Tree</b>							<b>Shrub</b>		<b>Grass</b>		<b>Special vegetation</b>		<b>Crops</b>		<b>Non-vegetated</b>	
<b>Holdridge Life Zone</b>	tropical broadleaf evergreen	tropical broadleaf deciduous	temperate broadleaf evergreen	temperate broadleaf deciduous	evergreen coniferous	deciduous coniferous	evergreen	deciduous	C3	C4	Tundra	Swamps	crops		urban	bare ground
1-30								70						30		

**Table A3.** Cross-walking table for ESA-CCI LC class 20 - Cropland, irrigated or post flooding. For LC class 20, no HLZ were assigned

	1	2	3	4	5	6	7	8	9	10	11	12	13	14	15	16
<b>Tree</b>							<b>Shrub</b>		<b>Grass</b>		<b>Special vegetation</b>		<b>Crops</b>		<b>Non-vegetated</b>	
<b>Holdridge Life Zone</b>	tropical broadleaf evergreen	tropical broadleaf deciduous	temperate broadleaf evergreen	temperate broadleaf deciduous	evergreen coniferous	deciduous coniferous	evergreen	deciduous	C3	C4	Tundra	Swamps	crops		urban	bare ground
1-30													100			



**Table A4.** Cross-walking table for ESA-CCI LC class 30 - Mosaic cropland (>50%) / natural vegetation (tree, shrub, herbaceous cover)(<50%).

	1	2	3	4	5	6	7	8	9	10	11	12	13	14	15	16
	Tree						Shrub		Grass		Special vegetation		Crops		Non-vegetated	
Holdridge Life Zone	tropical broadleaf evergreen	tropical broadleaf deciduous	temperate broadleaf evergreen	temperate broadleaf deciduous	evergreen coniferous	deciduous coniferous	evergreen	deciduous	C3	C4	Tundra	Swamps	crops		urban	bare ground
1-6											20	20	60			
7-9									40				60			
10					10				30				60			
11,12					30				10				60			
13,14									40				60			
15				5	5			20	10				60			
16				7.5	7.5			10	15				60			
17,18				20				10	10				60			
19									40				60			
20							20		20				60			
21,22				10	10			10	10				60			
23,24				10	10			20					60			
25									40				60			
26							20		20				60			
27		20					10		10				60			
28		10					15		15				60			
29	15						10		15				60			
30	20							10	10				60			

**Table A5.** Cross-walking table for ESA-CCI LC class 40 - Mosaic natural vegetation (tree, shrub, herbaceous cover)(>50%) / cropland(<50%)

	1	2	3	4	5	6	7	8	9	10	11	12	13	14	15	16
	Tree						Shrub		Grass		Special vegetation		Crops		Non-vegetated	
Holdridge Life Zone	tropical broadleaf evergreen	tropical broadleaf deciduous	temperate broadleaf evergreen	temperate broadleaf deciduous	evergreen coniferous	deciduous coniferous	evergreen	deciduous	C3	C4	Tundra	Swamps	crops		urban	bare ground
1,2											35	30	35			
3-5											30	35	35			
6											25	40	35			
7									60				40			
8					10				50				40			
9,10					15				45				40			
11					20				40				40			
12					30			20	10				40			
13				10	10			10	30				40			
14,15				20	20			10	10				40			
16				25	20				15				40			
17				25	25				10				40			
18				30	30								40			
19									60				40			
20							35		25				40			
21			20		15		15		10				40			
22			25		10		15		10				40			
23,24			20		20		20						40			
25									60				40			
26							30		30				40			
27		10					50						40			
28		40					20						40			
29	40						20						40			
30	50						10						40			



**Table A6.** Cross-walking table for ESA-CCI LC class 50 - Tree cover, broadleaved, evergreen, closed to open (>15%)

	1	2	3	4	5	6	7	8	9	10	11	12	13	14	15	16
<b>Holdridge Life Zone</b>	<b>Tree</b> tropical broadleaf evergreen	tropical broadleaf deciduous	temperate broadleaf evergreen	temperate broadleaf deciduous	evergreen coniferous	deciduous coniferous	<b>Shrub</b> evergreen	deciduous	<b>Grass</b> C3	C4	<b>Special vegetation</b> Tundra	Swamps	<b>Crops</b> crops		<b>Non-vegetated</b> urban	bare ground
1-6			12.5				12.5				75					
7-18			90	10												
19-24			100													
25-30	100															

**Table A7.** Cross-walking table for ESA-CCI LC class 60 - Tree cover, broadleaved, deciduous, closed to open (>15%)

	1	2	3	4	5	6	7	8	9	10	11	12	13	14	15	16
<b>Holdridge Life Zone</b>	<b>Tree</b> tropical broadleaf evergreen	tropical broadleaf deciduous	temperate broadleaf evergreen	temperate broadleaf deciduous	evergreen coniferous	deciduous coniferous	<b>Shrub</b> evergreen	deciduous	<b>Grass</b> C3	C4	<b>Special vegetation</b> Tundra	Swamps	<b>Crops</b> crops		<b>Non-vegetated</b> urban	bare ground
1-6							100									
7-24				70			15	15								
25-30		70					15	15								

**Table A8.** Cross-walking table for ESA-CCI LC class 61 - Tree cover, broadleaved, deciduous, closed (>40%)

	1	2	3	4	5	6	7	8	9	10	11	12	13	14	15	16
<b>Holdridge Life Zone</b>	<b>Tree</b> tropical broadleaf evergreen	tropical broadleaf deciduous	temperate broadleaf evergreen	temperate broadleaf deciduous	evergreen coniferous	deciduous coniferous	<b>Shrub</b> evergreen	deciduous	<b>Grass</b> C3	C4	<b>Special vegetation</b> Tundra	Swamps	<b>Crops</b> crops		<b>Non-vegetated</b> urban	bare ground
1-6							85	15								
7-24				70			15	15								
25-30		70					15	15								

**Table A9.** Cross-walking table for ESA-CCI LC class 62 - Tree cover, broadleaved, deciduous, open (15-40%)

	1	2	3	4	5	6	7	8	9	10	11	12	13	14	15	16
<b>Holdridge Life Zone</b>	<b>Tree</b> tropical broadleaf evergreen	tropical broadleaf deciduous	temperate broadleaf evergreen	temperate broadleaf deciduous	evergreen coniferous	deciduous coniferous	<b>Shrub</b> evergreen	deciduous	<b>Grass</b> C3	C4	<b>Special vegetation</b> Tundra	Swamps	<b>Crops</b> crops		<b>Non-vegetated</b> urban	bare ground
1-6							65	35								
7-24				30			25	45								
25-30		30					25	45								



**Table A10.** Cross-walking table for ESA-CCI LC class 70 - Tree cover, needleleaved, evergreen, closed to open (>15%) and LC class 71 - Tree cover, needleleaved, evergreen, closed (>40%)

	1	2	3	4	5	6	7	8	9	10	11	12	13	14	15	16
	Tree						Shrub		Grass		Special vegetation		Crops	Non-vegetated		
Holdridge Life Zone	tropical broadleaf evergreen	tropical broadleaf deciduous	temperate broadleaf evergreen	temperate broadleaf deciduous	evergreen coniferous	deciduous coniferous	evergreen	deciduous	C3	C4	Tundra	Swamps	crops		urban	bare ground
1-6					35	35	15		15							
7-18					70		10	5	15							
19-24			35		35		10	5	15							
25-30					70		10	5	15							

**Table A11.** Cross-walking table for ESA-CCI LC class 72 - Open (15-40%) needleleaved deciduous or evergreen forest (>5m)

	1	2	3	4	5	6	7	8	9	10	11	12	13	14	15	16
	Tree						Shrub		Grass		Special vegetation		Crops	Non-vegetated		
Holdridge Life Zone	tropical broadleaf evergreen	tropical broadleaf deciduous	temperate broadleaf evergreen	temperate broadleaf deciduous	evergreen coniferous	deciduous coniferous	evergreen	deciduous	C3	C4	Tundra	Swamps	crops		urban	bare ground
1-6					15	15	25		45							
7-18					30		20	5	45							
19-24			15		15		20	5	45							
25-30					30		20	5	45							

**Table A12.** Cross-walking table for ESA-CCI LC class 80 - Tree cover, needleleaved, deciduous, closed to open (>15%)

	1	2	3	4	5	6	7	8	9	10	11	12	13	14	15	16
	Tree						Shrub		Grass		Special vegetation		Crops	Non-vegetated		
Holdridge Life Zone	tropical broadleaf evergreen	tropical broadleaf deciduous	temperate broadleaf evergreen	temperate broadleaf deciduous	evergreen coniferous	deciduous coniferous	evergreen	deciduous	C3	C4	Tundra	Swamps	crops		urban	bare ground
1-30						50	5	15	30							

**Table A13.** Cross-walking table for ESA-CCI LC class 81 - Treecover, needleleaved, deciduous, closed (>40%)

	1	2	3	4	5	6	7	8	9	10	11	12	13	14	15	16
	Tree						Shrub		Grass		Special vegetation		Crops	Non-vegetated		
Holdridge Life Zone	tropical broadleaf evergreen	tropical broadleaf deciduous	temperate broadleaf evergreen	temperate broadleaf deciduous	evergreen coniferous	deciduous coniferous	evergreen	deciduous	C3	C4	Tundra	Swamps	crops		urban	bare ground
1-30						70		15	15							

**Table A14.** Cross-walking table for ESA-CCI LC class 82 - Tree cover, needleleaved, deciduous, open (15-40%)

	1	2	3	4	5	6	7	8	9	10	11	12	13	14	15	16
	Tree						Shrub		Grass		Special vegetation		Crops	Non-vegetated		
Holdridge Life Zone	tropical broadleaf evergreen	tropical broadleaf deciduous	temperate broadleaf evergreen	temperate broadleaf deciduous	evergreen coniferous	deciduous coniferous	evergreen	deciduous	C3	C4	Tundra	Swamps	crops		urban	bare ground
1-30						30	5	20	45							



**Table A15.** Cross-walking table for ESA-CCI LC class 90 - Tree cover, mixed leaf type (broadleaved and needleleaved)

	1	2	3	4	5	6	7	8	9	10	11	12	13	14	15	16
	Tree						Shrub		Grass		Special vegetation		Crops	Non-vegetated		
Holdridge Life Zone	tropical broadleaf evergreen	tropical broadleaf deciduous	temperate broadleaf evergreen	temperate broadleaf deciduous	evergreen coniferous	deciduous coniferous	evergreen	deciduous	C3	C4	Tundra	Swamps	crops	urban	bare ground	
1-12				20	70				10							
13-24				70	20				10							
25-30	45	45							10							

**Table A16.** Cross-walking table for ESA-CCI LC class 100 - Mosaic tree and shrub (>50%) / herbaceous cover(<50%)

	1	2	3	4	5	6	7	8	9	10	11	12	13	14	15	16
	Tree						Shrub		Grass		Special vegetation		Crops	Non-vegetated		
Holdridge Life Zone	tropical broadleaf evergreen	tropical broadleaf deciduous	temperate broadleaf evergreen	temperate broadleaf deciduous	evergreen coniferous	deciduous coniferous	evergreen	deciduous	C3	C4	Tundra	Swamps	crops	urban	bare ground	
1					30		30				30	10				
2,3					30		25				25	20				
4-6					30		20				20	30				
7-9				20	20		20		40							
10				25	25		20		30							
11				30	30		20		20							
12				30	30		25		15							
13				15	15			35	35							
14				20	20			30	30							
15				25	25			25	25							
16-18				25	25			30	20							
19,20			30				30		40							
21,22			35				35		30							
23,24			40				30		30							
25		20					50		30							
26		25					50		25							
27		30					45		25							
28		40					35		25							
29		60					20		20							
30		70					15		15							

**Table A17.** Cross-walking table for ESA-CCI LC class 110 - Mosaic herbaceous cover (>50%) / tree and shrub (<50%)

	1	2	3	4	5	6	7	8	9	10	11	12	13	14	15	16
	Tree						Shrub		Grass		Special vegetation		Crops	Non-vegetated		
Holdridge Life Zone	tropical broadleaf evergreen	tropical broadleaf deciduous	temperate broadleaf evergreen	temperate broadleaf deciduous	evergreen coniferous	deciduous coniferous	evergreen	deciduous	C3	C4	Tundra	Swamps	crops	urban	bare ground	
1-6							50				45	5				
7				10	10		20		60							
8				10	20		10		60							
9				25	25				50							
10				30	30				40							
11,12				35	35				30							
13				15	15				70							
14,15				20	10				70							
16				30				10	60							
17,18				35				15	50							
19			15				15		70							
20			10				20		70							
21			20				10		70							
22			30				10		60							
23,24			35				15		50							
25		15					15		70							
26		20					10		70							
27		25					15		60							
28		30						10	60							
29		40						10	50							
30		50						10	40							



**Table A18.** Cross-walking table for ESA-CCI LC class 120 - Shrubland

	1	2	3	4	5	6	7	8	9	10	11	12	13	14	15	16
	Tree						Shrub		Grass		Special vegetation		Crops		Non-vegetated	
Holdridge Life Zone	tropical broadleaf evergreen	tropical broadleaf deciduous	temperate broadleaf evergreen	temperate broadleaf deciduous	evergreen coniferous	deciduous coniferous	evergreen	deciduous	C3	C4	Tundra	Swamps	crops		urban	bare ground
1-6							40				55	5				
7-12							10	50	40							
13							70		30							
14							40	30	30							
15							20	60	20							
16							20	70	10							
17,18							10	80	10							
19							10		90							
20							50		50							
21							90		10							
22							80	10	10							
23,24							100									
25							10	10	80							
26,27							20	60	20							
28							10	70	20							
29,30							10	80	10							

**Table A19.** Cross-walking table for ESA-CCI LC class 121 - Evergreen shrubland and LC class 122 - Deciduous Shrubland

	1	2	3	4	5	6	7	8	9	10	11	12	13	14	15	16
	Tree						Shrub		Grass		Special vegetation		Crops		Non-vegetated	
Holdridge Life Zone	tropical broadleaf evergreen	tropical broadleaf deciduous	temperate broadleaf evergreen	temperate broadleaf deciduous	evergreen coniferous	deciduous coniferous	evergreen	deciduous	C3	C4	Tundra	Swamps	crops		urban	bare ground
1-6							40				55	5				
7-12							60		40							
13,14							70		30							
15							80		20							
16-18							90		10							
19							10		90							
20							50		50							
21,22							90		10							
23,24							100									
25							20		80							
26-28							80		20							
29,30							90		10							

**Table A20.** Cross-walking table for ESA-CCI LC class 122 - Evergreen shrubland and LC class 122 - Deciduous Shrubland

	1	2	3	4	5	6	7	8	9	10	11	12	13	14	15	16
	Tree						Shrub		Grass		Special vegetation		Crops		Non-vegetated	
Holdridge Life Zone	tropical broadleaf evergreen	tropical broadleaf deciduous	temperate broadleaf evergreen	temperate broadleaf deciduous	evergreen coniferous	deciduous coniferous	evergreen	deciduous	C3	C4	Tundra	Swamps	crops		urban	bare ground
1-6								40			55	5				
7-12								60	40							
13,14								70	30							
15								80	20							
16-18								90	10							
19								10	90							
20								50	50							
21,22								90	10							
23,24								100								
25								80	20							
26-28								80	20							
29,30								90	10							



**Table A21.** Cross-walking table for ESA-CCI LC class 130 - Grassland

	1	2	3	4	5	6	7	8	9	10	11	12	13	14	15	16
	Tree						Shrub		Grass		Special vegetation		Crops	Non-vegetated		
Holdridge Life Zone	tropical broadleaf evergreen	tropical broadleaf deciduous	temperate broadleaf evergreen	temperate broadleaf deciduous	evergreen coniferous	deciduous coniferous	evergreen	deciduous	C3	C4	Tundra	Swamps	crops	urban	bare ground	
1-6											90	10				
7-13									100							
14							5		95							
15								7.5	92.5							
16								10	90							
17								12.5	87.5							
18								15	85							
19									100							
20,21							5		95							
22							7.5		92.5							
23,24							10		90							
25									100							
26							5		95							
27							5	5	90							
28								10	90							
29								12.5	87.5							
30								15	85							

**Table A22.** Cross-walking table for ESA-CCI LC class 140 - Lichens and mosses

	1	2	3	4	5	6	7	8	9	10	11	12	13	14	15	16
	Tree						Shrub		Grass		Special vegetation		Crops	Non-vegetated		
Holdridge Life Zone	tropical broadleaf evergreen	tropical broadleaf deciduous	temperate broadleaf evergreen	temperate broadleaf deciduous	evergreen coniferous	deciduous coniferous	evergreen	deciduous	C3	C4	Tundra	Swamps	crops	urban	bare ground	
1-6											90	10				
7-30									100							



**Table A23.** Cross-walking table for ESA-CCI LC class 150 - Sparse vegetation (tree, shrub, herbaceouscover)(<15%)

	1	2	3	4	5	6	7	8	9	10	11	12	13	14	15	16
	Tree						Shrub		Grass		Special vegetation		Crops	Non-vegetated		
Holdridge Life Zone	tropical broadleaf evergreen	tropical broadleaf deciduous	temperate broadleaf evergreen	temperate broadleaf deciduous	evergreen coniferous	deciduous coniferous	evergreen	deciduous	C3	C4	Tundra	Swamps	crops	urban	bare ground	
1-6											50	10				40
7-12							10		40							50
13				5	5		5		35							50
14				5	5		10		30							50
15				5	5			10	30							50
16				5	5			20	20							50
17,18				10	10			20	10							50
19							5		45							50
20,21			5				5		40							50
22			5				10		35							50
23			10				10		30							50
24			15				15		20							50
25							5	5	40							50
26,27		10					5	5	30							50
28,29		10						20	20							50
30	10							20	20							50

**Table A24.** Cross-walking table for ESA-CCI LC class 151 - Sparse tree (<15%)

	1	2	3	4	5	6	7	8	9	10	11	12	13	14	15	16
	Tree						Shrub		Grass		Special vegetation		Crops	Non-vegetated		
Holdridge Life Zone	tropical broadleaf evergreen	tropical broadleaf deciduous	temperate broadleaf evergreen	temperate broadleaf deciduous	evergreen coniferous	deciduous coniferous	evergreen	deciduous	C3	C4	Tundra	Swamps	crops	urban	bare ground	
1-6											50	10				40
7-12							10		40							50
13				5	5				40							50
14,15				5	10				35							50
16				10	5				35							50
17,18				10	10				30							50
19-21			5						45							50
22			10						40							50
23			15						35							50
24			20						30							50
25		10							40							50
26-29		15							35							50
30	15								35							50



**Table A25.** Cross-walking table for ESA-CCI LC class 152 - Sparse shrub (<15%)

	1	2	3	4	5	6	7	8	9	10	11	12	13	14	15	16
	Tree						Shrub		Grass		Special vegetation		Crops		Non-vegetated	
Holdridge Life Zone	tropical broadleaf evergreen	tropical broadleaf deciduous	temperate broadleaf evergreen	temperate broadleaf deciduous	evergreen coniferous	deciduous coniferous	evergreen	deciduous	C3	C4	Tundra	Swamps	crops		urban	bare ground
1							5				45	10				40
2-6							10				40	10				40
7-10							10		40							50
11,12							20		30							50
13,14							10		40							50
15,16								15	35							50
17,18								20	30							50
19							5		45							50
20,21							10		40							50
22,23							15		35							50
24							20		30							50
25							5		45							50
26							10		40							50
27							7.5	7.5	35							50
28,29								15	35							50
30								20	30							50

**Table A26.** Cross-walking table for ESA-CCI LC class 153 - Sparse herbaceous cover (<15%)

	1	2	3	4	5	6	7	8	9	10	11	12	13	14	15	16
	Tree						Shrub		Grass		Special vegetation		Crops		Non-vegetated	
Holdridge Life Zone	tropical broadleaf evergreen	tropical broadleaf deciduous	temperate broadleaf evergreen	temperate broadleaf deciduous	evergreen coniferous	deciduous coniferous	evergreen	deciduous	C3	C4	Tundra	Swamps	crops		urban	bare ground
1-6											40	10				50
7-30									50							50



**Table A27.** Cross-walking table for ESA-CCI LC class 160 - Tree cover, flooded, fresh or brakish water

	1	2	3	4	5	6	7	8	9	10	11	12	13	14	15	16
	Tree						Shrub		Grass		Special vegetation		Crops		Non-vegetated	
Holdridge Life Zone	tropical broadleaf evergreen	tropical broadleaf deciduous	temperate broadleaf evergreen	temperate broadleaf deciduous	evergreen coniferous	deciduous coniferous	evergreen	deciduous	C3	C4	Tundra	Swamps	crops		urban	bare ground
1-6				10							45	45				
7-18				70								30				
19-24			70									30				
25-30	35	35										30				

**Table A28.** Cross-walking table for ESA-CCI LC class 170 - Tree cover, flooded, saline water

	1	2	3	4	5	6	7	8	9	10	11	12	13	14	15	16
	Tree						Shrub		Grass		Special vegetation		Crops		Non-vegetated	
Holdridge Life Zone	tropical broadleaf evergreen	tropical broadleaf deciduous	temperate broadleaf evergreen	temperate broadleaf deciduous	evergreen coniferous	deciduous coniferous	evergreen	deciduous	C3	C4	Tundra	Swamps	crops		urban	bare ground
1-6					40		30				10	20				
7-12				20				60				20				
13-18				30				50				20				
19-24			60				10	10				20				
25-30	80											20				



**Table A29.** Cross-walking table for ESA-CCI LC class 180 - Shrub or herbaceous cover, flooded, fresh / saline / brakish water

	1	2	3	4	5	6	7	8	9	10	11	12	13	14	15	16
	Tree						Shrub		Grass		Special vegetation		Crops	Non-vegetated		
Holdridge Life Zone	tropical broadleaf evergreen	tropical broadleaf deciduous	temperate broadleaf evergreen	temperate broadleaf deciduous	evergreen coniferous	deciduous coniferous	evergreen	deciduous	C3	C4	Tundra	Swamps	crops	urban	bare ground	
1-6											95	5				
7								10				90				
8							15	15	20			50				
9							20	20	20			40				
10-12							20	20	20			40				
13								20	20			60				
14								25	25			50				
15								30	30			40				
16								35	35			30				
17,18								45	15			40				
19,20							30	40	30							
21,22							40	40	20							
23							40	50	10							
24							30	60	10							
25							30	30	40							
26							30	40	30							
27							40	40	20							
28							40	50	10							
29							70	30								
30							90	10								

**Table A30.** Cross-walking table for ESA-CCI LC class 190 - Urban

	1	2	3	4	5	6	7	8	9	10	11	12	13	14	15	16
	Tree						Shrub		Grass		Special vegetation		Crops	Non-vegetated		
Holdridge Life Zone	tropical broadleaf evergreen	tropical broadleaf deciduous	temperate broadleaf evergreen	temperate broadleaf deciduous	evergreen coniferous	deciduous coniferous	evergreen	deciduous	C3	C4	Tundra	Swamps	crops	urban	bare ground	
1-30																100

**Table A31.** Cross-walking table for ESA-CCI LC class 200 - Bare areas, LC class 201 - Consolidated bare areas and LC class 202 - Unconsolidated bare areas.

	1	2	3	4	5	6	7	8	9	10	11	12	13	14	15	16
	Tree						Shrub		Grass		Special vegetation		Crops	Non-vegetated		
Holdridge Life Zone	tropical broadleaf evergreen	tropical broadleaf deciduous	temperate broadleaf evergreen	temperate broadleaf deciduous	evergreen coniferous	deciduous coniferous	evergreen	deciduous	C3	C4	Tundra	Swamps	crops	urban	bare ground	
1-30																100



## Appendix B

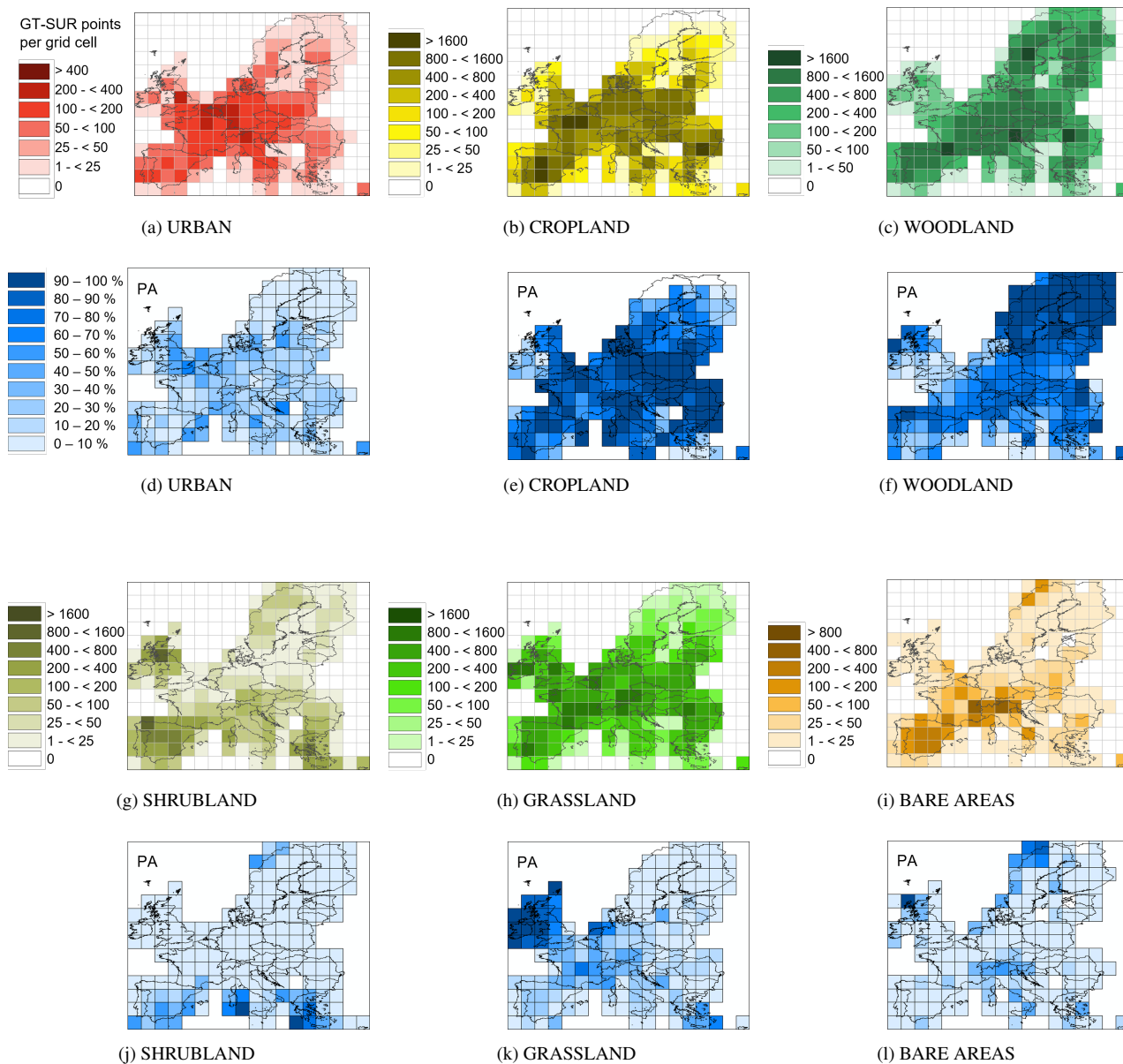


**Figure B1.** Total count of GT-SUR points per 2.5° grid cell (a-c; g-i) and producer's accuracy for the individual LULC groups (d-f;j-l) for filter set 5 (dominant LULC group occupies > 50% per LANDMATE PFT grid cell)

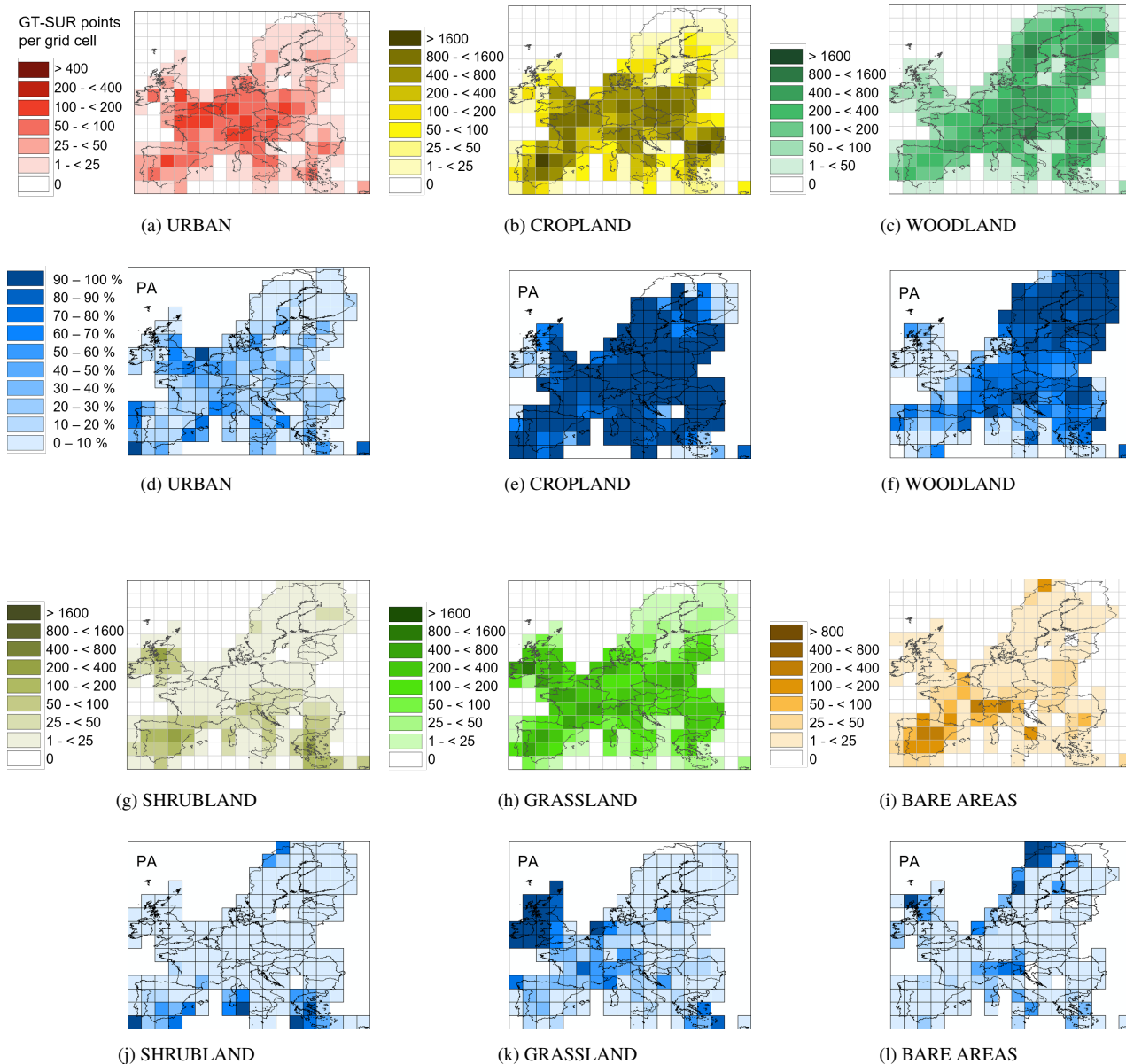


**Figure B2.** Total count of GT-SUR points per 2.5° grid cell (a-c; g-i) and producer's accuracy for the individual LULC groups (d-f;j-l) for filter set 7 (dominant LULC group occupies > 70% per LANDMATE PFT grid cell)



	1	2	3	4	5	6	7	SUM	UA
1	3234	806	1063	178	1769	120	407	7577	42.68
2	6625	67374	22298	5444	28559	4185	2485	136970	49.19
3	2414	5081	88064	8989	12818	1527	5544	124437	70.77
4	624	5316	4637	5498	1789	439	1487	19790	27.78
5	1411	4515	8063	6082	20763	1767	1643	44244	46.93
6	82	199	200	830	567	1810	460	4148	43.64
7	3	4	49	277	276	530	314	1453	21.61
SUM	14393	83295	124374	27298	66541	10378	12340		
PA	22.47	80.887	70.81	20.14	31.20	17.44	2.54	OA:	55.24

**Table B1.** Confusion matrix for LANDMATE PFT filter set 1 - Dominant LULC group occupies a minimum of 10 % of a LANDMATE PFT grid cell

	1	2	3	4	5	6	7	SUM	UA
1	3234	806	1063	178	1769	120	407	7577	42.68
2	6625	67374	22298	5444	28559	4185	2485	136970	49.19
3	2414	5081	88064	8989	12818	1527	5544	124437	70.77
4	624	5316	4637	5498	1789	439	1487	19790	27.78
5	1411	4515	8063	6082	20763	1767	1643	44244	46.93
6	82	199	200	830	567	1810	460	4148	43.64
7	3	4	49	277	276	530	314	1453	21.61
SUM	14393	83295	124374	27298	66541	10378	12340		
PA	22.47	80.887	70.81	20.14	31.20	17.44	2.54	OA:	55.24

**Table B2.** Confusion matrix for LANDMATE PFT filter set 2 - Dominant LULC group occupies a minimum of 20 % of a LANDMATE PFT grid cell



	1	2	3	4	5	6	7	SUM	UA
1	3221	793	1041	174	1748	117	404	7498	42.96
2	6596	67323	22210	5395	28488	4168	2457	136637	49.27
3	2377	5034	87838	8903	12750	1511	5483	123896	70.90
4	615	5280	4484	5363	1748	425	1401	19316	27.76
5	1401	4485	7961	5983	20716	1754	1559	43859	47.23
6	78	187	186	798	552	1799	452	4052	44.40
7	3	4	47	276	275	530	310	1445	21.45
SUM	14291	83106	123767	26892	66277	10304	12066		
PA	22.54	81.01	70.97	19.94	31.26	17.46	2.57	OA:	55.41

**Table B3.** Confusion matrix for LANDMATE PFT filter set 3 - Dominant LULC group occupies a minimum of 30 % of a LANDMATE PFT grid cell

	1	2	3	4	5	6	7	SUM	UA
1	3079	715	904	152	1597	109	364	6920	44.49
2	6263	66184	20069	4795	27209	4034	2304	130858	50.58
3	2061	4045	83073	7509	11168	1274	5030	114160	72.77
4	501	4813	3013	4235	1392	329	742	15025	28.19
5	1238	4031	6748	5091	19572	1571	1219	39470	49.59
6	54	123	122	606	469	1681	425	3480	48.30
7	2	2	40	254	258	517	252	1325	19.02
SUM	13198	79913	113969	22642	61665	9515	10336		
PA	23.33	82.82	72.89	18.70	31.74	17.67	2.44	OA:	57.22

**Table B4.** Confusion matrix for LANDMATE PFT filter set 4 - Dominant LULC group occupies a minimum of 40 % of a LANDMATE PFT grid cell



	1	2	3	4	5	6	7	SUM	UA
1	2632	499	676	117	1218	84	292	5518	47.70
2	5482	62499	15269	3772	23519	3737	1913	116191	53.79
3	1510	2215	71799	5277	7767	853	4284	93705	76.62
4	362	3865	1752	2689	915	206	350	10139	26.52
5	933	2992	4373	3605	16306	1227	893	30329	53.76
6	31	61	62	292	321	1375	392	2534	54.26
7	1	0	29	110	214	233	70	657	10.65
SUM	10951	72131	93960	15862	50260	7715	8194		
PA	24.03	86.65	76.41	16.95	32.44	17.82	0.85	OA:	60.74

**Table B5.** Confusion matrix for LANDMATE PFT filter set 5 - Dominant LULC group occupies a minimum of 50 % of a LANDMATE PFT grid cell

	1	2	3	4	5	6	7	SUM	UA
1	2123	284	464	85	844	67	231	4098	51.81
2	4436	56963	10802	2887	19016	3314	1556	98974	57.55
3	1025	978	57212	2949	4699	488	3345	70696	80.93
4	194	2459	967	1713	518	122	240	6213	27.57
5	628	1847	2584	2333	12497	798	630	21317	58.62
6	14	27	34	104	181	1022	339	1721	59.38
7	1	0	18	40	153	87	25	324	7.72
SUM	8421	62558	72081	10111	37908	5898	6366		
PA	25.21	91.06	79.37	16.94	32.97	17.33	0.39	OA:	64.70

**Table B6.** Confusion matrix for LANDMATE PFT filter set 6 - Dominant LULC group occupies a minimum of 60 % of a LANDMATE PFT grid cell



	1	2	3	4	5	6	7	SUM	UA
1	1684	167	311	53	568	44	185	3012	55.91
2	3288	49624	7217	2088	14351	2840	1145	80553	61.60
3	414	255	30158	806	1745	177	1910	35465	85.04
4	40	793	458	988	191	42	160	2672	36.98
5	410	1053	1363	1415	9113	478	425	14257	63.92
6	5	11	15	61	104	768	302	1266	60.66
7	1	0	9	19	99	50	9	187	4.81
SUM	5842	51903	39531	5430	26171	4399	4136		
PA	28.83	95.61	76.29	18.20	34.82	17.46	0.22	OA:	67.20

**Table B7.** Confusion matrix for LANDMATE PFT filter set 7 - Dominant LULC group occupies a minimum of 70 % of a LANDMATE PFT grid cell

	1	2	3	4	5	6	7	SUM	UA
1	1261	83	208	29	369	32	138	2120	59.48
2	2009	38997	4002	1296	9321	2239	745	58609	66.54
3	32	21	3201	54	195	8	108	3619	88.45
4	10	74	198	442	51	9	106	890	49.66
5	241	518	640	691	5957	240	229	8516	69.95
6	3	5	10	39	62	533	268	920	57.93
7	1	0	6	8	53	17	6	91	6.59
SUM	3557	39698	8265	2559	16008	3078	1600		
PA	35.45	98.23	38.73	17.27	37.21	17.32	0.38	OA:	67.41

**Table B8.** Confusion matrix for LANDMATE PFT filter set 8 - Dominant LULC group occupies a minimum of 80 % of a LANDMATE PFT grid cell



	1	2	3	4	5	6	7	SUM	UA
1	808	44	111	14	207	16	89	1289	62.68
2	592	17167	877	414	2601	1043	269	22963	74.76
3	1	1	47	1	1	0	14	65	72.31
4	2	7	28	74	11	1	10	133	55.64
5	40	81	108	181	1358	83	58	1909	71.14
6	3	1	7	20	28	338	230	627	53.91
7	0	0	1	2	2	1	1	7	14.29
SUM	1446	17301	1179	706	4208	1482	671		
PA	55.88	99.23	3.99	10.48	32.27	22.81	0.15	OA:	73.33

**Table B9.** Confusion matrix for LANDMATE PFT filter set 9 - Dominant LULC group occupies a minimum of 90 % of a LANDMATE PFT grid cell

	1	2	3	4	5	6	7	SUM	UA
1	252	10	28	0	40	8	51	389	64.78
2	22	565	16	7	52	14	20	696	81.18
3	0	0	0	0	0	0	0	0	/
4	0	0	0	0	0	0	0	0	/
5	0	1	4	14	48	6	1	74	64.86
6	2	0	4	7	9	112	156	290	38.62
7	0	0	0	0	0	0	0	0	/
SUM	276	576	52	28	149	140	228		
PA	91.30	98.09	0.00	0.00	32.21	80.00	0.00	OA:	67.43

**Table B10.** Confusion matrix for LANDMATE PFT filter set 10 - Dominant LULC group occupies 100 % of a LANDMATE PFT grid cell



540 *Author contributions.* VR conceptualized the paper outline and objective with the support of DR, PH and JB. VR and PH developed the cross-walking procedure and the corresponding cross-walking tables. PH developed the required translation software for the cross-walking procedure. VR developed the accuracy assessment design for the LANDMATE PFT map supported by BB. VR conducted the accuracy assessment and the visualization of results. VR wrote the original draft of the paper, VR, PH, DR, JB, and BB reviewed and edited the draft. VR wrote the final paper

*Competing interests.* The authors declare that they have no conflict of interest.

545 *Acknowledgements.* This work was financed within the framework of the Helmholtz Institute for Climate Service Science (HICSS), a co-operation between Climate Service Center Germany (GERICS) and Universität Hamburg, Germany and conducted as part of the project LANDMATE (Modelling human LAND surface modifications and its feedbacks on local and regional cliMATE). We acknowledge the support of LUCAS by WCRP-CORDEX as a Flagship Pilot Study. We acknowledge the E-OBS dataset from the EU-FP6 project UERRA (<http://www.uerra.eu>) and the Copernicus Climate Change Service, and the data providers in the ECA&D project (<https://www.ecad.eu>).  
550 We thank the European Space Agency (ESA) for making the Land cover products publicly available. Special thanks go to the FPS LUCAS partners for providing useful comments in order to improve the dataset.



## References

- Alkama, R. and Cescatti, A.: Biophysical climate impacts of recent changes in global forest cover, *Science*, 351, 600–604, 2016.
- Bégué, A., Arvor, D., Bellon, B., Betbeder, J., De Abelleira, D., PD Ferraz, R., Lebourgeois, V., Lelong, C., Simões, M., and R Verón, S.:  
555 Remote sensing and cropping practices: A review, *Remote Sensing*, 10, 99, 2018.
- Belda, M., Halenka, T., Huszar, P., Karlicky, J., and Nováková, T.: Do we need urban parameterization in high resolution regional climate simulations?, in: *AGU Fall Meeting Abstracts*, vol. 2018, pp. A21L–2878, 2018.
- Bojinski, S., Verstraete, M., Peterson, T. C., Richter, C., Simmons, A., and Zemp, M.: The concept of essential climate variables in support of climate research, applications, and policy, *Bulletin of the American Meteorological Society*, 95, 1431–1443, 2014.
- 560 Bonan, G. B.: Forests and climate change: forcings, feedbacks, and the climate benefits of forests, *science*, 320, 1444–1449, 2008.
- Bonan, G. B., Levis, S., Kergoat, L., and Oleson, K. W.: Landscapes as patches of plant functional types: An integrating concept for climate and ecosystem models, *Global Biogeochemical Cycles*, 16, 5–1, 2002.
- Bontemps, S., Defourny, P., Radoux, J., Van Bogaert, E., Lamarche, C., Achard, F., Mayaux, P., Boettcher, M., Brockmann, C., Kirches, G., et al.: Consistent global land cover maps for climate modelling communities: current achievements of the ESA's land cover CCI, in:  
565 *Proceedings of the ESA living planet symposium*, Edinburgh, pp. 9–13, 2013.
- Box, E. O.: Plant functional types and climate at the global scale, *Journal of Vegetation Science*, 7, 309–320, 1996.
- Bright, R. M., Zhao, K., Jackson, R. B., and Cherubini, F.: Quantifying surface albedo and other direct biogeophysical climate forcings of forestry activities, *Global Change Biology*, 21, 3246–3266, 2015.
- Burke, M. and Emerick, K.: Adaptation to climate change: Evidence from US agriculture, *American Economic Journal: Economic Policy*, 8,  
570 106–40, 2016.
- Chapin Iii, F., McGuire, A., Randerson, J., Pielke, R., Baldocchi, D., Hobbie, S. E., Roulet, N., Eugster, W., Kasischke, E., Rastetter, E., et al.: Arctic and boreal ecosystems of western North America as components of the climate system, *Global Change Biology*, 6, 211–223, 2000.
- Chen, X., Zhang, X.-S., and Li, B.-L.: The possible response of life zones in China under global climate change, *Global and Planetary  
575 Change*, 38, 327–337, 2003.
- Conrad, O., Bechtel, B., Bock, M., Dietrich, H., Fischer, E., Gerlitz, L., Wehberg, J., Wichmann, V., and Böhner, J.: System for automated geoscientific analyses (SAGA) v. 2.1. 4., *Geoscientific Model Development Discussions*, 8, 2015.
- Cornes, R. C., van der Schrier, G., van den Besselaar, E. J., and Jones, P. D.: An ensemble version of the E-OBS temperature and precipitation data sets, *Journal of Geophysical Research: Atmospheres*, 123, 9391–9409, 2018.
- 580 Daly, C., Helmer, E. H., and Quiñones, M.: Mapping the climate of puerto rico, vieques and culebra, *International Journal of Climatology: A Journal of the Royal Meteorological Society*, 23, 1359–1381, 2003.
- Daniel, M., Lemonsu, A., Déqué, M., Somot, S., Alias, A., and Masson, V.: Benefits of explicit urban parameterization in regional climate modeling to study climate and city interactions, *Climate Dynamics*, 52, 2745–2764, 2019.
- Davin, E. L., Rechid, D., Breil, M., Cardoso, R. M., Coppola, E., Hoffmann, P., Jach, L. L., Katragkou, E., de Noblet-Ducoudré, N., Radtke, K., et al.: Biogeophysical impacts of forestation in Europe: first results from the LUCAS (Land Use and Climate Across Scales) regional  
585 climate model intercomparison, *Earth System Dynamics*, 11, 183–200, 2020.
- Di Gregorio, A.: Land cover classification system: classification concepts and user manual: LCCS, vol. 2, Food & Agriculture Org., 2005.



- Dierckx, W., Sterckx, S., Benhadj, I., Livens, S., Duhoux, G., Van Achteren, T., Francois, M., Mellab, K., and Saint, G.: PROBA-V mission for global vegetation monitoring: standard products and image quality, *International Journal of Remote Sensing*, 35, 2589–2614, 2014.
- 590 Donlon, C., Berruti, B., Buongiorno, A., Ferreira, M.-H., Féménias, P., Frerick, J., Goryl, P., Klein, U., Laur, H., Mavrocordatos, C., et al.: The global monitoring for environment and security (GMES) sentinel-3 mission, *Remote Sensing of Environment*, 120, 37–57, 2012.
- d’Andrimont, R., Yordanov, M., Martinez-Sanchez, L., Eiselt, B., Palmieri, A., Dominici, P., Gallego, J., Reuter, H. I., Joebges, C., Lemoine, G., et al.: Harmonised LUCAS in-situ land cover and use database for field surveys from 2006 to 2018 in the European Union, *Scientific Data*, 7, 1–15, 2020.
- 595 ESA: Land Cover CCI Product User Guide Version 2, Tech. rep., European Space Agency, [maps.elie.ucl.ac.be/CCI/viewer/download/ESACCI-LC-Ph2-PUGv2\\_2.0.pdf](https://maps.elie.ucl.ac.be/CCI/viewer/download/ESACCI-LC-Ph2-PUGv2_2.0.pdf), 2017.
- ESA: Land cover CCI product user guide version 2, Tech. Report, pp. p–105, 2017.
- ESA, E. A. P.: Available online: [http://envisat.esa.int/handbooks/asar\\_CNTR.html](http://envisat.esa.int/handbooks/asar_CNTR.html) (accessed on 27 January 2020), 2002.
- Foody, G. M.: Status of land cover classification accuracy assessment, *Remote sensing of environment*, 80, 185–201, 2002.
- 600 Ge, J., Qi, J., Lofgren, B. M., Moore, N., Torbick, N., and Olson, J. M.: Impacts of land use/cover classification accuracy on regional climate simulations, *Journal of Geophysical Research: Atmospheres*, 112, 2007.
- Harris, I., Jones, P., Osborn, T., and Lister, D.: Updated high-resolution grids of monthly climatic observations – the CRU TS3.10 Dataset, *International Journal of Climatology*, 34, 623–642, <https://doi.org/10.1002/joc.3711>, 2014.
- Hartley, A., MacBean, N., Georgievski, G., and Bontemps, S.: Uncertainty in plant functional type distributions and its impact on land surface models, *Remote Sensing of Environment*, 203, 71–89, 2017.
- 605 Hastings, D. A. and Emery, W. J.: The advanced very high resolution radiometer (AVHRR)-A brief reference guide, *Photogrammetric Engineering and Remote Sensing*, 58, 1183–1188, 1992.
- Hoffmann, P., Katzfey, J., McGregor, J., and Thatcher, M.: Bias and variance correction of sea surface temperatures used for dynamical downscaling, *Journal of Geophysical Research: Atmospheres*, 121, 12–877, 2016.
- 610 Hoffmann, P., Reinhart, V., Rechid, D., de Noblet-Ducoudré, N., Davin, E., Asmus, C., Bechtel, B., Böhner, J., Katragou, E., and Luysaert, S.: High-resolution land-use land-cover change data for regional climate modelling applications over Europe - Part 2: Historical and future changes, *ESSD*, submitted.
- Holdridge, L. R. et al.: Life zone ecology., *Life zone ecology.*, 1967.
- Hua, T., Zhao, W., Liu, Y., Wang, S., and Yang, S.: Spatial consistency assessments for global land-cover datasets: A comparison among GLC2000, CCI LC, MCD12, GLOBCOVER and GLCNMO, *Remote Sensing*, 10, 1846, 2018.
- 615 Hurtt, G. C., Chini, L. P., Frolking, S., Betts, R., Feddema, J., Fischer, G., Fisk, J., Hibbard, K., Houghton, R., Janetos, A., et al.: Harmonization of land-use scenarios for the period 1500–2100: 600 years of global gridded annual land-use transitions, wood harvest, and resulting secondary lands, *Climatic change*, 109, 117, 2011.
- Jung, M., Henkel, K., Herold, M., and Churkina, G.: Exploiting synergies of global land cover products for carbon cycle modeling, *Remote Sensing of Environment*, 101, 534–553, 2006.
- 620 Karthikeyan, L., Chawla, I., and Mishra, A. K.: A review of remote sensing applications in agriculture for food security: Crop growth and yield, irrigation, and crop losses, *Journal of Hydrology*, 586, 124 905, 2020.
- Khatun, K., Imbach, P., and Zamora, J.: An assessment of climate change impacts on the tropical forests of Central America using the Holdridge Life Zone (HLZ) land classification system, *iForest-Biogeosciences and Forestry*, 6, 183, 2013.



- 625 Kueppers, L. M., Snyder, M. A., and Sloan, L. C.: Irrigation cooling effect: Regional climate forcing by land-use change, *Geophysical Research Letters*, 34, 2007.
- Lattanzi, F. A.: C3/C4 grasslands and climate change, in: *Grassland Science in Europe*, pp. 3–13, 2010.
- Lavorel, S., Díaz, S., Cornelissen, J. H. C., Garnier, E., Harrison, S. P., McIntyre, S., Pausas, J. G., Pérez-Harguindeguy, N., Roumet, C., and Urcelay, C.: Plant functional types: are we getting any closer to the Holy Grail?, in: *Terrestrial ecosystems in a changing world*, pp. 630 149–164, Springer, 2007.
- Lawrence, D. and Vandecar, K.: Effects of tropical deforestation on climate and agriculture, *Nature climate change*, 5, 27–36, 2015.
- Li, W., MacBean, N., Ciais, P., Defourny, P., Lamarche, C., Bontemps, S., Houghton, R. A., and Peng, S.: Gross and net land cover changes in the main plant functional types derived from the annual ESA CCI land cover maps (1992–2015), 2018.
- Lobell, D., Bala, G., and Duffy, P.: Biogeophysical impacts of cropland management changes on climate, *Geophysical Research Letters*, 33, 635 2006.
- Lu, Y. and Kueppers, L. M.: Surface energy partitioning over four dominant vegetation types across the United States in a coupled regional climate model (Weather Research and Forecasting Model 3–Community Land Model 3.5), *Journal of Geophysical Research: Atmospheres*, 117, 2012.
- Lugo, A. E., Brown, S. L., Dodson, R., Smith, T. S., and Shugart, H. H.: The Holdridge life zones of the conterminous United States in 640 relation to ecosystem mapping, *Journal of biogeography*, 26, 1025–1038, 1999.
- Mahmood, R., Pielke Sr, R. A., Hubbard, K. G., Niyogi, D., Dirmeyer, P. A., McAlpine, C., Carleton, A. M., Hale, R., Gameda, S., Beltrán-Przekurat, A., et al.: Land cover changes and their biogeophysical effects on climate, *International journal of climatology*, 34, 929–953, 2014.
- Maisongrande, P., Duchemin, B., and Dedieu, G.: VEGETATION/SPOT: an operational mission for the Earth monitoring; presentation of 645 new standard products, *International Journal of Remote Sensing*, 25, 9–14, 2004.
- Marconcini, M., Metz-Marconcini, A., Üreyen, S., Palacios-Lopez, D., Hanke, W., Bachofer, F., Zeidler, J., Esch, T., Gorelick, N., Kakarla, A., et al.: Outlining where humans live, the World Settlement Footprint 2015, *Scientific Data*, 7, 1–14, 2020.
- Olofsson, P., Foody, G. M., Herold, M., Stehman, S. V., Woodcock, C. E., and Wulder, M. A.: Good practices for estimating area and assessing accuracy of land change, *Remote Sensing of Environment*, 148, 42–57, 2014.
- 650 Ottosen, T.-B., Lommen, S. T., and Skjøth, C. A.: Remote sensing of cropping practice in Northern Italy using time-series from Sentinel-2, *Computers and Electronics in Agriculture*, 157, 232–238, 2019.
- Pau, S., Edwards, E. J., and Still, C. J.: Improving our understanding of environmental controls on the distribution of C3 and C4 grasses, *Global Change Biology*, 19, 184–196, 2013.
- Perugini, L., Caporaso, L., Marconi, S., Cescatti, A., Quesada, B., de Noblet-Ducoudre, N., House, J. I., and Arneth, A.: Biophysical effects 655 on temperature and precipitation due to land cover change, *Environmental Research Letters*, 12, 053002, 2017.
- Poulter, B., Ciais, P., Hodson, E., Lischke, H., Maignan, F., Plummer, S., and Zimmermann, N.: Plant functional type mapping for earth system models, *Geoscientific Model Development*, 4, 993, 2011.
- Poulter, B., MacBean, N., Hartley, A., Khlystova, I., Arino, O., Betts, R., Bontemps, S., Boettcher, M., Brockmann, C., Defourny, P., et al.: Plant functional type classification for earth system models: results from the European Space Agency’s Land Cover Climate Change 660 Initiative, *Geoscientific Model Development*, 8, 2315–2328, 2015.
- Rechid, D., Davin, E., de Noblet-Ducoudré, N., and Katragkou, E.: CORDEX Flagship Pilot Study" LUCAS-Land Use & Climate Across Scales"-a new initiative on coordinated regional land use change and climate experiments for Europe, EGUGA, p. 13172, 2017.



- Reinhart, V., Fonte, C. C., Hoffmann, P., Bechtel, B., Rechid, D., and Böhner, J.: Comparison of ESA climate change initiative land cover to CORINE land cover over Eastern Europe and the Baltic States from a regional climate modeling perspective, *International Journal of Applied Earth Observation and Geoinformation*, 94, 102 221, 2021a.
- 665 Reinhart, V., Hoffmann, P., and Rechid, D.: LANDMATE PFT land cover dataset for Europe 2015 (Version 1.0), [https://doi.org/10.26050/WGCC/LM\\_PFT\\_LandCov\\_EUR2015\\_v1.0](https://doi.org/10.26050/WGCC/LM_PFT_LandCov_EUR2015_v1.0), 2021b.
- Richardson, A. D., Keenan, T. F., Migliavacca, M., Ryu, Y., Sonnentag, O., and Toomey, M.: Climate change, phenology, and phenological control of vegetation feedbacks to the climate system, *Agricultural and Forest Meteorology*, 169, 156–173, 2013.
- 670 Rufin, P., Frantz, D., Ernst, S., Rabe, A., Griffiths, P., Özdoğan, M., and Hostert, P.: Mapping cropping practices on a national scale using intra-annual landsat time series binning, *Remote Sensing*, 11, 232, 2019.
- Saad, R., Koellner, T., and Margni, M.: Land use impacts on freshwater regulation, erosion regulation, and water purification: a spatial approach for a global scale level, *The International Journal of Life Cycle Assessment*, 18, 1253–1264, 2013.
- Santos-Alamillos, F., Pozo-Vázquez, D., Ruiz-Arias, J., and Tovar-Pescador, J.: Influence of land-use misrepresentation on the accuracy of WRF wind estimates: Evaluation of GLCC and CORINE land-use maps in southern Spain, *Atmospheric Research*, 157, 17–28, 2015.
- 675 Sertel, E., Robock, A., and Ormeci, C.: Impacts of land cover data quality on regional climate simulations, *International Journal of Climatology*, 30, 1942–1953, 2010.
- Siebert, S., Döll, P., Hoogeveen, J., Faures, J.-M., Frenken, K., and Feick, S.: Development and validation of the global map of irrigation areas, *Hydrology and Earth System Sciences*, 9, 535–547, 2005.
- 680 Skov, F. and Svenning, J.-C.: Potential impact of climatic change on the distribution of forest herbs in Europe, *Ecography*, 27, 366–380, 2004.
- Stehman, S. V.: Sampling designs for accuracy assessment of land cover, *International Journal of Remote Sensing*, 30, 5243–5272, 2009.
- Sulla-Menashe, D. and Friedl, M. A.: User guide to collection 6 MODIS land cover (MCD12Q1 and MCD12C1) product, USGS: Reston, VA, USA, pp. 1–18, 2018.
- 685 Szelepcsényi, Z., Breuer, H., and Sümegei, P.: The climate of Carpathian Region in the 20th century based on the original and modified Holdridge life zone system, *Central European Journal of Geosciences*, 6, 293–307, 2014.
- Szelepcsényi, Z., Breuer, H., Kis, A., Pongrácz, R., and Sümegei, P.: Assessment of projected climate change in the Carpathian Region using the Holdridge life zone system, *Theoretical and applied climatology*, 131, 593–610, 2018.
- Tatli, H. and Dalfes, H. N.: Defining Holdridge’s life zones over Turkey, *International Journal of Climatology*, 36, 3864–3872, 2016.
- 690 Tatli, H. and Dalfes, H. N.: Analysis of temporal diversity of precipitation along with biodiversity of Holdridge life zones, *Theoretical and Applied Climatology*, 144, 391–400, 2021.
- Thompson, C., Beringer, J., Chapin III, F. S., and McGuire, A. D.: Structural complexity and land-surface energy exchange along a gradient from arctic tundra to boreal forest, *Journal of Vegetation Science*, 15, 397–406, 2004.
- Vilar, L., Garrido, J., Echavarría, P., Martínez-Vega, J., and Martín, M. P.: Comparative analysis of CORINE and climate change initiative land cover maps in Europe: Implications for wildfire occurrence estimation at regional and local scales, *International Journal of Applied Earth Observation and Geoinformation*, 78, 102–117, 2019.
- 695 Wei, Y., Liu, S., Huntzinger, D., Michalak, A., Viovy, N., Post, W., Schwalm, C., Schaefer, K., Jacobson, A., LU, C., Tian, H., Ricciuto, D., Cook, R., Mao, J., and Shi, X.: NACP MsTMIP: Global and North American Driver Data for Multi-Model Intercomparison, <https://doi.org/10.3334/ORNLDAAC/1220>, 2014.



- 700 Wilhelm, C., Rechid, D., and Jacob, D.: Interactive coupling of regional atmosphere with biosphere in the new generation regional climate system model REMO-iMOVE, *Geoscientific Model Development*, 7, 1093–1114, <https://doi.org/10.5194/gmd-7-1093-2014>, 2014.
- Winter, J. M., Pal, J. S., and Eltahir, E. A.: Coupling of integrated biosphere simulator to regional climate model version 3, *Journal of Climate*, 22, 2743–2757, 2009.
- Wulder, M. A., Franklin, S. E., White, J. C., Linke, J., and Magnussen, S.: An accuracy assessment framework for large-area land cover classification products derived from medium-resolution satellite data, *International Journal of Remote Sensing*, 27, 663–683, 2006.
- 705 Wullschleger, S. D., Epstein, H. E., Box, E. O., Euskirchen, E. S., Goswami, S., Iversen, C. M., Kattge, J., Norby, R. J., van Bodegom, P. M., and Xu, X.: Plant functional types in Earth system models: past experiences and future directions for application of dynamic vegetation models in high-latitude ecosystems, *Annals of botany*, 114, 1–16, 2014.
- Yang, Y., Xiao, P., Feng, X., and Li, H.: Accuracy assessment of seven global land cover datasets over China, *ISPRS Journal of Photogrammetry and Remote Sensing*, 125, 156–173, 2017.
- 710 Yue, T., Liu, J., Jørgensen, S. E., Gao, Z., Zhang, S., and Deng, X.: Changes of Holdridge life zone diversity in all of China over half a century, *Ecological Modelling*, 144, 153–162, 2001.
- Yue, T. X., Fan, Z. M., Liu, J. Y., and Wei, B. X.: Scenarios of major terrestrial ecosystems in China, *ecological modelling*, 199, 363–376, 2006.